

Prepared for:

Rijkswaterstaat, RIKZ

Influence of collapsed revetments on dune erosion

Large-scale model tests

Report

February, 2007

Prepared for:

Rijkswaterstaat, RIKZ

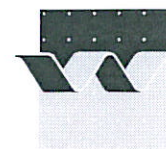
Influence of collapsed revetments on dune erosion

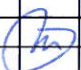

Large-scale model tests

E.M. Coeveld and M.R.A. van Gent

Report

February, 2007



CLIENT:	Rijkswaterstaat, RIKZ							
TITLE:	Influence of collapsed revetments on dune erosion Large-scale model tests							
ABSTRACT:	<p>Knowledge to take the influence of collapsed dune revetments (e.g. seaside boulevards, buildings, dune foot revetments, etc.) into account in the prediction of dune erosion is missing. In the current safety assessment method of the Dutch dunes, revetments in a cross-shore dune profile that fail are considered not to affect (positively or negatively) dune erosion under storm surge conditions compared to a dune profile without these elements. However, this assumption has never been verified with physical model tests. The objective of this study is to verify this assumption by performing large-scale physical model tests.</p> <p>In total, four large-scale tests were carried out. One test was performed for a collapsing dune foot revetment and three tests for a seawall with a low dune behind. The tests with a seawall were carried out with a stable seawall, a collapsing seawall and an absent seawall. These tests were performed at a depth scale of $n_d = 6$ with the same hydraulic conditions as in the dune erosion tests earlier in 2006. A wave height of $H_{m0} = 9$ m (prototype), wave period of $T_p = 12$ s (prototype) and sediment with a diameter of $D_{50} = 200$ μm were applied in the tests. Bed profile, wave and flow velocity measurements were carried out in four tests with two configurations of dune revetments.</p> <p>From the test with the stable seawall it becomes clear that a scour hole in front of a vertical revetment rapidly develops towards an equilibrium depth. The maximum scour depth relative to the initial water depth is somewhat larger than the maximum scour depth found in existing data on sloping revetments.</p> <p>Based on the results of the tests, it can be concluded that for the tested geometries there are no important effects of a collapsed revetment or seawall on dune erosion in a 2D situation. It appeared that the erosion process for dunes with revetment is very similar to the erosion process of dunes without revetment, e.g. the rapid retreat of the dune face in the beginning of the storm and the logarithmic time-development of the erosion volume above the still water level can also be observed at dunes with revetment. Consequently, the dune erosion volume does not increase because of these elements and does not significantly decrease either. In a 3D situation however, effects of collapsed dune revetments might still be present. Further analyses of the data and additional investigations to 3D aspects are necessary for the development of future guidelines.</p>							
REFERENCES:	WL Delft Hydraulics' proposal: MCI-16024/H4357/MvG, dated March 24 th , 2006. Acceptance of proposal: RIKZ/2006/05323, dated May 11 th , 2006.							
VER	AUTHORS		DATE	REMARKS	REVIEW		APPROVED BY	
0	M.R.A. van Gent		November 2006	Draft	J. van de Graaff	JvdG	W.M.K. Tilmans	
	E.M. Coeveld							
1	M.R.A. van Gent		Februari 2007	Final	J. van de Graaff	JvdG	W.M.K. Tilmans 	
	E.M. Coeveld							
PROJECT NUMBER:			H4731					
KEYWORDS:			Dune, dune erosion, physical model test, dune foot revetment, scour					
NUMBER OF PAGES:								
CONFIDENTIAL:			<input type="checkbox"/> YES, until		<input checked="" type="checkbox"/> NO			
STATUS:			<input type="checkbox"/> PRELIMINARY		<input type="checkbox"/> DRAFT		<input checked="" type="checkbox"/> FINAL	

Contents

List of Figures

List of Tables

List of Photographs

List of Symbols

1	Introduction	1
2	Set up of physical model tests	5
2.1	Introduction	5
2.2	Model description	5
2.2.1	Revetments.....	5
2.2.2	Coastal profile	7
2.2.3	Delta flume.....	7
2.2.4	Scale relations	7
2.2.5	Model set up.....	9
2.3	Test conditions	11
2.4	Measurements	13
2.4.1	Bed profile	13
2.4.2	Wave conditions and water depth.....	15
2.4.3	Other measurements	16
3	Results of physical model tests	19
3.1	Introduction	19
3.2	Wave conditions and water depth	19
3.3	Profile changes and dune erosion volumes.....	21
3.3.1	Test T11: reference dune profile with revetment.....	21
3.3.2	Test T12: scour hole at vertical wall.....	26

3.3.3	Test T13: relatively low dune with revetment.....	28
3.3.4	Test T14: Test T13 without revetment.....	30
3.4	Other measurements	34
4	Further interpretations of results	35
4.1	Introduction.....	35
4.2	Effects of hard elements in safety assessment.....	35
4.3	Scour holes in safety assessment	36
5	Conclusions and recommendations.....	39
5.1	Conclusions	39
5.2	Recommendations	40

References

Appendices

- A Tables**
- B Figures**
- C Photographs**

List of Figures

Figures (in the text):

Figure 1.1	Definition of reference profile	4
Figure 1.2	Definition of characteristic erosion volumes and (erosion) points in a cross-shore profile.....	4
Figure 2.1	Overview of hard coastal defence systems	6
Figure 2.2	Cross-shore coastal profile with relatively low seaside part of dune	7
Figure 3.1	Wave heights over coastal profile from pressure measurements	20
Figure 3.2	Development of retreat of dune face in time in Tests T01, and T11	24
Figure 3.3	Development of erosion volume in time in Tests T01 and T11	25
Figure 3.4	Development of volume and of maximum depth of scour hole in time in Test T12.....	27
Figure 3.5	Definition sketch of scour hole.....	28
Figure 3.6	Development of erosion volumes in time in Test T13.....	30
Figure 3.7	Development of retreat of dune in time in Tests T01, T13 and T14	31
Figure 3.8	Development of erosion volumes in time in Tests T13 and T14.....	33
Figure 3.9	Development of erosion volumes in time in Tests T01, T13 and T14.....	34
Figure 4.1	Schematic top-view of effects of hard elements on dune erosion at location where (a) revetment partially collapsed, and (b) seawall and sandy dune come together (according to Figure 4.54 in TAW, 1995)	36
Figure 4.2	Profile development in Test T01 of research programme H0298 (WL Delft Hydraulics, 1987a).....	37

Figures (in Appendix B):

Figure B.1	Desired initial profile (outer geometry) and positions of instruments fixed at flume walls in Tests T11, T12, T13 and T14
Figure B.2	Revetments in Tests T11, T12 and T13
Figure B.3	Development of average cross-shore profiles; Test T11
Figure B.4	Comparison of average cross-shore profiles of tests with equal hydraulic conditions and initial profiles (outer geometry); Tests T01 and T11
Figure B.5	Development of average cross-shore profiles; Test T12
Figure B.6	Development of average cross-shore profiles; Test T13
Figure B.7	Development of average cross-shore profiles; Test T14
Figure B.8	Comparison of average cross-shore profiles of tests with equal hydraulic conditions and initial profiles (outer geometry); Tests T13 and T14

- Figure B.9 Comparison of average (horizontally translated) cross-shore profiles of tests with equal hydraulic conditions; Tests T01 and T14
- Figure B.10 Incident wave height exceedance curve and energy density spectra; T11E
- Figure B.11 Incident wave height exceedance curve and energy density spectra; T12E
- Figure B.12 Incident wave height exceedance curve and energy density spectra; T13E
- Figure B.13 Incident wave height exceedance curve and energy density spectra; T14E
- Figure B.14 Energy density spectra in pressure sensors

List of Tables

Tables (in the text):

Table 2.1 Characteristics of structure elements used in the tests	10
Table 2.2 Overview of tests carried out.....	10
Table 2.3 Test conditions with generated hydraulic conditions at wave board ($T_{m-1,0} = T_p / 1.1$)	12
Table 2.4 Positions of pressure sensors	16
Table 3.1 Dune erosion volumes above still water level and increase in erosion volumes in Tests T01 and T11	25
Table 3.2 Volume and maximum depth of scour hole in Test T12.....	27
Table 3.3 Erosion volumes above still water level and total erosion volumes in Test T13 ...	30
Table 3.4 Erosion volumes above still water level and total erosion volumes in Test T14 ...	33

Tables (in Appendix A):

Table A.1	Parts of profile that were measured in m from the wave board
Table A.2	Incident wave conditions measured with wave height meters WHM01, WHM02 and WHM03
Table A.3	Wave conditions measured with wave height meters WHM01, WHM02 and WHM03
Table A.4	Incident wave conditions measured with pressure sensor PS01 and flow velocity meter EMS01
Table A.5	Wave conditions measured with pressure sensors PS01 – PS03
Table A.6	Wave conditions measured with pressure sensors PS04 – PS06
Table A.7	Wave conditions measured with pressure sensors PS07 – PS09
Table A.8	Measured water temperatures
Table A.9	Masses and densities of structure elements

List of Photographs

Photographs (in Appendix C):

- | | |
|------------|--|
| Photo C.1 | Revetment around dune face and dune top before Test T11 |
| Photo C.2 | Revetment before Test T12 |
| Photo C.3 | Revetment before Test T13 |
| Photo C.4 | Dune before Test T14 |
| Photo C.5 | Amphibious profile follower, flow velocity meter and pressure sensor |
| Photo C.6 | Photographs for stereo video before Test T11 |
| Photo C.7 | Photographs for stereo video at end of Test T13 |
| Photo C.8 | Wave attack at revetment at beginning of Test T11 |
| Photo C.9 | Wave attack at revetment during collapse of revetment on dune face in Test T11 |
| Photo C.10 | Dune and revetment after collapse of revetment on dune face in Test T11 |
| Photo C.11 | Dune and revetment after Test T11 |
| Photo C.12 | Wave attack at revetment in Test T12 |
| Photo C.13 | Dune and revetment after Test T12 |
| Photo C.14 | Wave attack at revetment in Test T13 |
| Photo C.15 | Dune and revetment after Test T13 |
| Photo C.16 | Dune, revetment and bed profile after Test T13 in dry flume |
| Photo C.17 | Wave attack at dune in Test T14 |
| Photo C.18 | Dune during and after Test T14 |

List of Symbols

Symbol	Unit	Meaning
a	-	Coefficient in Equation 2.7 to determine fall velocity w
A	m^3/m^1	Dune erosion volume per linear meter dune above storm surge level (or still water level)
A_2	m^3/m^1	Dune erosion volume per linear meter dune below storm surge level (or still water level)
b	-	Coefficient in Equation 2.7 to determine fall velocity w
c	-	Coefficient in Equation 2.7 to determine fall velocity w
D	m	Grain size diameter
D_{10}	m	Grain size diameter such that 10 % of the grains by mass are smaller than $D = D_{10}$
D_{50}	m	Grain size diameter such that 50 % of the grains by mass are smaller than $D = D_{50}$
D_{90}	m	Grain size diameter such that 90 % of the grains by mass are smaller than $D = D_{90}$
D_n	m	Characteristic size of structure elements in revetment
Fr	-	Froude number
g	m/s^2	Gravitational acceleration ($= 9.81 \text{ m}/\text{s}^2$)
h	m	Water depth
h_i	m	Initial water depth
H	m	Wave height
H_{m0}	m	Significant wave height based on wave spectrum
L	m	Length measure
M	kg	Mass of structure elements in revetment
n_A	-	Erosion area (or volume per linear meter) scale factor
n_d	-	Depth scale factor
n_l	-	Horizontal length scale factor
n_w	-	Fall velocity scale factor
O_{90}	m	Aperture in geotextile for which 90 % of grains with diameter $D = O_{90}$ remain on fabric
P	m	Erosion point P (intersection of initial profile and storm surge level)
Q	m	Erosion point Q (intersection of erosion profile and storm surge level)
S	-	Profile steepness factor
S_0	-	Profile steepness factor applied in the model
S_I	-	Desired profile steepness factor

Symbol	Unit	Meaning
$S_{m-1,0}$	-	Wave steepness at deep water based on spectral wave period ($= 2 \cdot \pi \cdot H_{m0} / g \cdot T_{m-1,0}^2$)
S_p	-	Wave steepness at deep water based on peak wave period ($= 2 \cdot \pi \cdot H_{m0} / g \cdot T_p^2$)
T	s	Wave period
$T_{m-1,0}$	s	Spectral wave period ($= m_{-1} / m_0$ with $m_n = \int f^n \cdot S(f) \cdot df$ in which f (Hz) is the frequency and S (m^2/Hz) is the variance density)
T_p	s	Peak wave period, defined as the period in an arbitrary wave spectrum with a global maximum of the spectral density
u	m/s	Flow velocity
w	m/s	Fall velocity of sediment with grain size $D = D_{50}$, in stagnant water
w_{50}	m/s	Fall velocity exceeded by 50 % (in mass) of sediment in stagnant water
x	m	Horizontal distance
y	m	Vertical distance
Δ	-	Relative buoyant density ($= (\rho_a - \rho_w) / \rho_w$)
ρ_a	kg/m ³	Density of structure elements
ρ_w	kg/m ³	Density of water

I Introduction

Background information

To allow for the five yearly safety assessment of the Dutch primary water defences the ‘Directoraat-Generaal Water’ of the Ministry ‘Verkeer en Waterstaat’ has commissioned the ‘Directoraat-Generaal Rijkswaterstaat’ to develop a new dune safety assessment method for the year 2006. With this new method it should primarily be possible to calculate dune erosion under normative hydraulic conditions taking effects of the wave period into account. Dune erosion calculations are expected to be based on new hydraulic boundary conditions that will also be defined in the year 2006 (in Dutch: ‘Hydraulische Randvoorwaarden 2006’ or ‘HR2006’). The ‘Directoraat-Generaal Rijkswaterstaat’, RIKZ, accepted (ref: RIKZ/2005/05707, dated July 7th, 2005) WL | Delft Hydraulics’ proposal (ref: MCI-10835/H4357/MvG, dated May 20th, 2005) to develop this new safety assessment method. The assignment included large-scale physical model tests in which the necessary insights into the effects of the wave period on dune erosion could be obtained. Additional tests were performed in which the attention was focussed on the processes relevant for dune erosion, especially those underlying the effects of the wave period.

In addition to the effects of the wave period on dune erosion, there are also knowledge gaps about the behaviour of hard structures (*e.g.* seaside boulevards, buildings, dune (foot) revetments, etc.) in sandy dunes, especially when they fail. In the current safety assessment method of the Dutch dunes collapsing hard structures in a cross-shore dune profile are considered not to affect (positively or negatively) dune erosion under storm surge conditions compared to a dune profile without these elements. However, this assumption has never been verified with physical model tests.

The ‘Directoraat-Generaal Rijkswaterstaat’, RIKZ, accepted (ref: RIKZ/2006/05323, dated May 11th, 2006) WL | Delft Hydraulics’ proposal (ref: MCI-16024/H4357/MvG, dated March 24th 2006) to perform additional large-scale dune erosion tests to gain insight into the effects of collapsed dune revetments on dune erosion. Besides, ‘Projectbureau Zeeweringen’ of ‘Rijkswaterstaat Zeeland’, accepted (ref: 4528, dated June 13th, 2006) WL | Delft Hydraulics’ proposal (ref: MCI-16019/H4357/MvG, dated March 24th 2006) to perform an additional large-scale dune erosion test for the same purpose. This test is also included in the present report.

Problem definition

An inventory of required knowledge on hard elements in a sandy coastal defence revealed a number of knowledge gaps of which the following 2D effects are considered to be the most important:

- The effects of a collapsed hard dune (foot) revetment on dune erosion under normative storm conditions for a) vertical structures or revetments and b) sloping revetments. A number of small- and large-scale dune erosion tests (*e.g.* WL | Delft Hydraulics, 1982a,

1983, 1987a and 1987b) have been performed in which revetments were applied. However, in these tests the revetments did not collapse under normative storm conditions.

- The depth of the scour hole at a vertical dune (foot) revetment. In the earlier dune erosion tests (*e.g.* WL | Delft Hydraulics, 1982a, 1983, 1987a and 1987b) scour holes at sloping revetments were investigated.

Besides, there are a number of 3D effects related to hard elements in a sandy coastal defence:

- The 3D aspects of a partly collapsed dune (foot) revetment
- The transition between a section of a dune with a dune revetment and a dune without a dune revetment.
- Various other situations in which hard elements interact with a sandy coast, like for instance the situation around the connection of a dune and a dike, or the situation around dunes landward of a dike with a limited capability to withstand high waters.

Objective

The objective of this study is to obtain knowledge of 2D effects of hard structures on dune erosion, especially for the following cases:

- The effect of a collapsed dune foot revetment on the dune erosion profile.
- The effect of a collapsed vertical seawall on the dune erosion profile.
- The effect of a stable vertical seawall on the depth of the scour hole.

The data obtained from these tests form a first important step to improve and extend the knowledge on relevant processes for the safety assessment of the Dutch primary water defences. This knowledge will be used in the development of future guidelines for the safety assessment, for example in the VTV of the year 2011.

Scope

In this study attention is focussed on the physical model tests which were set up to provide information on the first two knowledge gaps mentioned in the problem definition. This report provides an overview of the data obtained from the tests including some brief analyses. Further analyses of the data and additional research to obtain knowledge about 3D effects of hard structures on dune erosion are foreseen in the development of future guidelines, but not included in the present study. The physical model tests do not directly provide data on the stability of a revetment itself.

Approach

The physical model is set up similar to the dune erosion tests carried out prior to the present tests (WL | Delft Hydraulics, 2006b). This facilitates a comparison of dune erosion in situations with and without revetments. The shape of the revetments do not refer to specific situations or locations in reality.

Project organisation

Project manager of this project is Dr M.R.A. van Gent and the project engineers are E.M. Coeveld and I. van der Werf (all from WL | Delft Hydraulics). On behalf of the Delft University of Technology, Dr J. van de Graaff is project advisor. The set up of the physical model tests was also discussed with Dr H.J. Steetzel on behalf of Alkyon Hydraulics Research & Consultancy and Prof. dr L.C. van Rijn of WL | Delft Hydraulics.

Reader's guide

In Chapter 2 the set up of the large-scale physical model tests is described. Chapter 3 describes the results of the tests. In Chapter 4 some further analyses are presented. Chapter 5 summarises the main conclusions.

The following definitions have been used in this report (in arbitrary order):

- The **VTV** (in Dutch: 'Voorschrift Toetsen Veiligheid') is the safety assessment regulation drawn up by the Dutch government for the five yearly safety assessment (prescribed in the Law on Water Defences) of the primary water defences by the administrators of those water defences, see Ministry of Transport, Public Works and Water Management (2004).
- The **earlier dune erosion tests** are the tests carried out prior to the present tests (see WL | Delft Hydraulics, 2006b) at the same depth scale and with the same sediment. **Test T01** was carried out with a wave period of $T_p = 4.90$ s, wave height of $H_{m0} = 1.5$ m and water depth of 4.5 m.
- The **flume** in which the large-scale physical model tests are carried out is the Delta flume of WL | Delft Hydraulics. The flume has an effective length, width and height of 225 m, 5 m and 7 m respectively. The wave generator is equipped with Active Reflection Compensation and 2nd order wave steering.
- The **profile** is the bed level below and above the still water level (beach and dune) in cross-shore direction.
- To indicate directions or orientations use is made of the following expressions:
 - The **seaward** direction is the direction from the dune top towards the wave board and the **landward** direction is the opposite direction.
 - The **cross-shore** profile is the profile in a direction along the flume axis.

The **reference profile** is a characteristic profile for the Dutch coast and has a dune top located at NAP +15 m. The slope of the dune face is 1:3 and ends at NAP +3 m. From thereon the slope is 1:20 to a level of NAP. From NAP to NAP -3 m the slope is 1:70. From that point on seaward the slope is 1:180, see Figure 1.1. The same profile was used in earlier dune erosion research (e.g. WL | Delft Hydraulics, 1982b) and derived by averaging the measured cross-shore profiles at a number of locations along the Dutch coast.

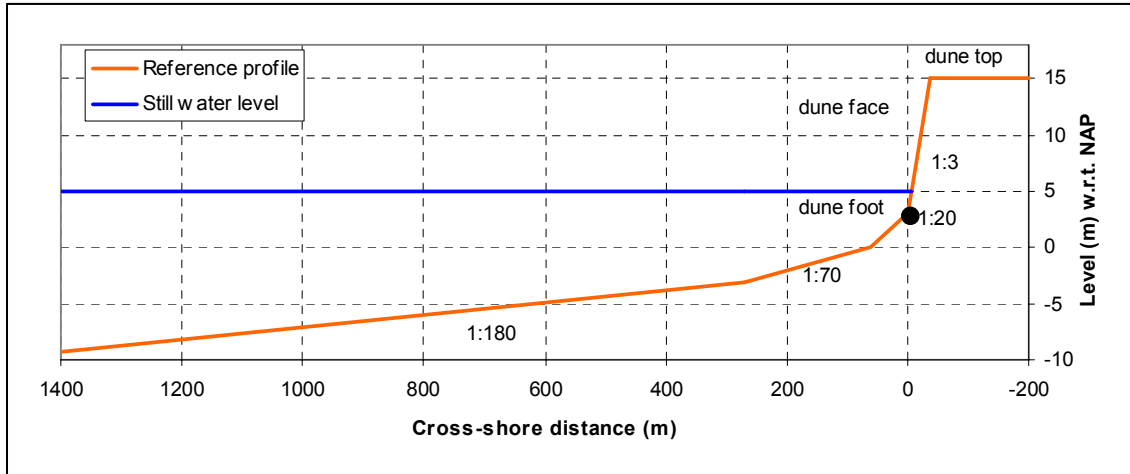


Figure 1.1 Definition of reference profile

- The **dune top** is the highest point of the dune, see Figure 1.1. The **dune face** is the steep part **seaward** of the dune top. The **dune foot** is the lower end of the dune face.
- The **erosion volume A** is the erosion volume per linear meter above still water (or storm surge) level based on the difference between the initial profile and the erosion profile after a storm event, see Figure 1.2. The **erosion volume A_2** is the erosion volume below still water level. The total dune erosion volume E is the sum of A and A_2 . The accretion volume can be expected entirely below the still water level.
- **Erosion point Q** is defined at the intersection of the erosion profile and the still water (or storm surge) level. **Point P** is defined at the intersection of the initial profile and the still water (or storm surge) level. The distance between point P and erosion point Q is a measure for the dune face retreat after a storm event.

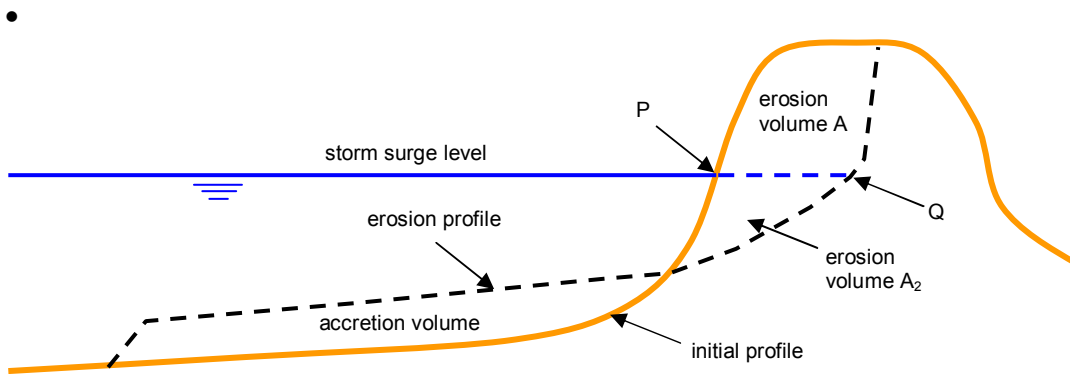


Figure 1.2 Definition of characteristic erosion volumes and (erosion) points in a cross-shore profile

2 Set up of physical model tests

2.1 Introduction

To gain insight into the effects of collapsed dune revetments on dune erosion, large-scale physical model tests were performed. The wave attack on characteristic cross-shore dune profiles with several revetments during a storm event was simulated.

In this chapter the set up of the physical model tests is described. Section 2.2 describes the characteristics of the dune profile with its revetment and the flume in which the profile is applied. Section 2.3 gives an overview of the test programme. The measurements carried out during the tests and the measurement devices used for this purpose are described in Section 2.4.

All values presented in this chapter are ‘model values’ (viz. measures of and results of measurements in the physical model in the Delta flume), unless they are specifically referred to as ‘prototype values’ (corresponding to a field situation).

2.2 Model description

2.2.1 Revetments

A wide variety of hard coastal defence systems can be found along the Dutch coast. They can be subdivided into the following categories (see Figure 2.1):

- Sea dike: a coastal defence system designed to withstand a normative storm event. A sea dike can be covered with sand at the seaward side or the landward side.
- Seawall: a vertical wall that acts as individual defence system or as part of a primary water defences.
- Dune foot revetments can have several goals: fixation of the sand of a dune, reduction of dune erosion under a storm event of limited size and duration (for example an event with a frequency of exceedance of 1/500 per year) or fully participation as a part of the sea defence for normative conditions. Most of the dune foot revetments are sloping elements made of asphalt or blocks of basalt or concrete. Some guidelines exist to determine the reduction of the erosion volume because of these revetments (TAW, 1995). These are only valid under the assumption that the revetment is strong enough to withstand the storm surge.

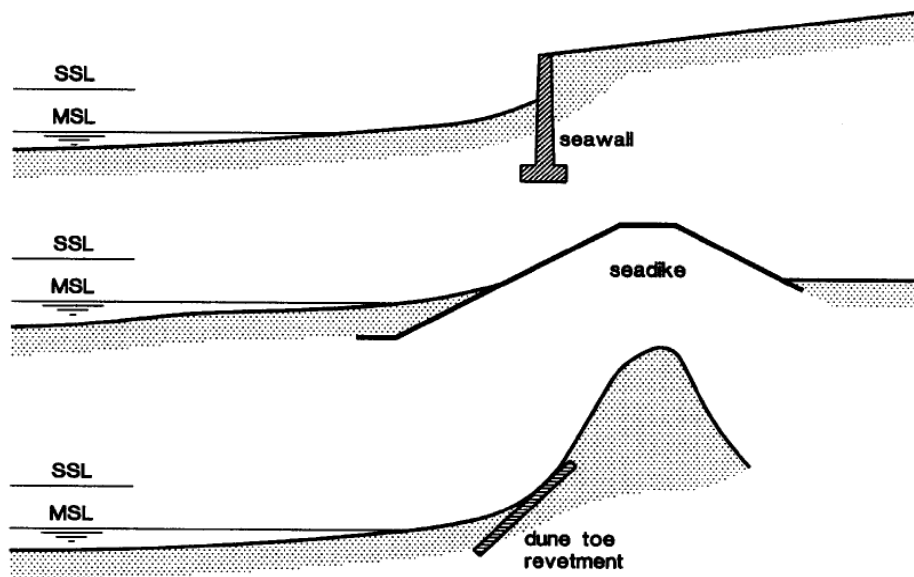


Figure 2.1 Overview of hard coastal defence systems

The expected size and depth of the scour hole seaward of the revetment caused by a normative storm event determines the construction depth of the revetment. The analysis of an extensive series of laboratory tests and field data reveals that the maximum depth of a scour hole can be approximated at the initial water depth at some distance from the dune foot (Van Rijn, 1998). For example, a storm surge level at NAP +4 m and an initial bed level at NAP +1 m would lead to a depth of the scour hole of about 3 m (until a level of NAP -2 m). The construction depth should then be at a level of about NAP -3 m taking some additional safety into account. For practical reasons it can be decided to construct the revetment at an even lower depth to prevent failure through undermining or to construct a falling apron in front of the dune foot revetment, so that the scour hole is moved further from the defence (TAW, 1995). It is not very useful to restrict the construction height of such a structure, because the additional costs are relatively low. Besides, a dune foot revetment with its top at about the storm surge level has no significant reducing effects on the total dune erosion. Thus, in order to have some dune erosion reducing effects by the dune foot revetment, it needs to be constructed until a level well above the storm surge level during a normative storm (around NAP +5 m), for example until a level of NAP +7 m. Nevertheless, erosion will still take place above this level, because of the wave run up. Failure of a dune foot revetment is caused by the undermining by a scour hole, or by the crumbling off of the top side of the revetment.

The sloping revetments are (traditionally) constructed of layers of asphalt or of a more flexible construction of piled up basalt or concrete blocks (with dimensions of about 0.5 m). The vertical revetments are constructed of basalt or concrete blocks reinforced with cement. Boulevards, roads or other pavements along the beaches are typically made of asphalt, bricks or concrete plates (with dimensions of about 1.5 to 2 m).

2.2.2 Coastal profile

Two configurations of cross-shore coastal profiles are used. The profile that was used in the first of the two tested configurations is based on the reference profile which is considered to be characteristic for the Dutch coast, see Figure 1.1. This strongly schematised profile consists of one dune with its dune top located at NAP +15 m. The slope of the dune face is 1:3 and ends at NAP +3 m. From thereon the slope is 1:20 to a level of NAP. From NAP to NAP -3 m the slope is 1:70. From that point on seaward the slope is 1:180. No banks or channels are present in the foreshore. For the second configuration, a somewhat different cross-shore coastal profile is used. The part under the still water level is similar to the first configuration, but around the still water level a vertical part is present just seaward of a relatively low horizontal part. This configuration is representing for instance a boulevard as can be found at some of the seaside resorts in The Netherlands, see Figure 2.2.

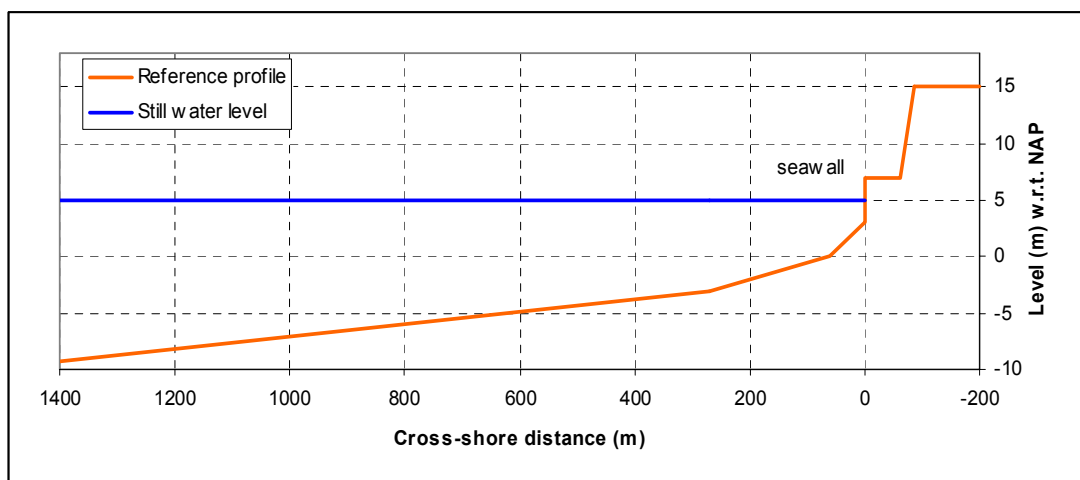


Figure 2.2 Cross-shore coastal profile with relatively low seaside part of dune

2.2.3 Delta flume

The wave flume in which the large-scale physical model tests were carried out is the Delta flume of WL | Delft Hydraulics. The flume has an effective length, width and height of 225 m, 5 m and 7 m respectively. The wave generator is equipped with Active Reflection Compensation and 2nd order wave steering. Irregular waves with a wave height up to 1.9 m can be generated depending on the water depth and the wave period. The scale at which the tests could be performed were restricted by the dimensions of the wave flume and on the capacity of the wave generator in the flume given the coastal profile and the hydraulic conditions expected during an extreme storm event along the Dutch coast.

2.2.4 Scale relations

Scaling relations exist for dune erosion processes (typically for the Dutch situation) and for the processes relevant for the stability of structure elements under wave attack. The scale relations can be used for the translation of a prototype situation to a model on a smaller (geometrical) scale and are briefly described hereafter. However, scaling relations for

situations in which the processes relevant for both aspects are combined are not known to exist. Especially the erosion process around the elements is difficult to simulate properly.

Dune erosion

The scale relations used to translate a prototype situation to a model that fits in the flume are derived by Vellinga (1986). Reference is also made to WL | Delft Hydraulics (2006a) for a comprehensive overview of the applied scale relations.

For a certain depth scale factor (n_d) and fall velocity scale factor (n_w) the desired profile steepness factor of the initial profile can be determined with (WL | Delft Hydraulics, 1982b):

$$S_1 = \frac{n_l}{n_d} = \left(\frac{n_d}{n_w^2} \right)^{0.28} \quad 2.1$$

in which n_l is the horizontal length scale factor. Ideally an undistorted profile is applied in the model, but since proper modelling of n_w in relation to n_d is difficult, one often ends with a value for the steepness factor of $S_l > 1$. However, the dimensions of the flume often require an even steeper profile, multiplied with a factor S_0 instead of the desired factor S_l .

Taking this profile steepness factor into account the dune erosion of an initial profile is thought to be properly simulated at a smaller scale in a wave flume. The erosion area (or volume per linear meter) scale factor is:

$$n_A = n_l \cdot n_d = n_d^2 \cdot \left(\frac{n_d}{n_w^2} \right)^{0.28} \quad 2.2$$

By multiplying the measured dune erosion volume (per linear meter) with n_A the prototype volume is obtained which applies for a prototype initial profile that is a factor S steeper than the reference profile:

$$S = \frac{S_0}{S_1} \quad 2.3$$

S_0 is the steepness factor that is applied in the model.

Structure elements in revetment

For the structure elements with which the revetment is constructed the scaling law of Froude is available to translate the sizes of the elements from a model to a prototype situation (and vice versa). The Froude scaling law dictates that the Froude number in the model is the same as in prototype. The Froude number is defined as:

$$Fr = \frac{u^2}{gL} \quad 2.4$$

in which u (m/s) is the velocity, g (m/s²) the gravitational acceleration and L (m) a length measure. This scaling law is valid for phenomena that are dominated by inertia and gravity, which is (partly) the case for the processes relevant for the stability in these model tests. Therefore, scaling according to the scaling law of Froude is often referred to as scaling on stability.

The stability parameter is defined as $H_s/\Delta D_n$, in which Δ (-) is the relative buoyant density ($= (\rho_a - \rho_w)/\rho_w$), D_n (m) is a characteristic size of the elements, ρ_a (kg/m³) is the armour density and ρ_w (kg/m³) is the water density. Using this relation the mass of the elements in the model, can be translated to prototype values using:

$$M_p = n_d^3 \cdot \frac{\rho_{a,p}}{\rho_{a,m}} \cdot \left(\frac{\Delta_p}{\Delta_m} \right)^{1/3} \cdot M_m \quad 2.5$$

in which M (kg) is the mass of an element and the subscripts m , p refer to model and prototype, respectively. The mass of an element can be related to the dimensions of an element:

$$M = \rho_a \cdot V \quad 2.6$$

where V (m³) is the volume of an element which equals the product of length, height and width. Differences in density are taken into account in this formulation. However, since the physical model represents an average or characteristic situation for the Dutch coast and not one specific situation, the prototype densities are not known exactly. Furthermore, the fact that the scale relations for dune erosion require a model distortion (viz. $n_d \neq n_l$) is not directly taken into account in Equation 2.5.

2.2.5 Model set up

A similar model set up was used as in the dune erosion tests prior to the present tests (see WL | Delft Hydraulics, 2006b). Several configurations of a dune in combination with a revetment were used in the tests. The sediment that was applied in the flume was compacted in layers of about 0.5 m. Table 2.1 shows some characteristics of the elements of the revetments used in the tests. The prototype characteristics are calculated with Equation 2.5 under the assumption that the densities of water and elements are equal in model and prototype. The dimensions of the model material were mainly determined by the available material on a model scale. Nevertheless, the corresponding prototype dimensions are not unrealistic.

Element	Location	Model		Prototype	
		Mass (kg)	Length · width · height (m · m · m)	Mass (kg)	Length · width · height (m · m · m)
Blocks	Dune face	1.9	0.1 · 0.1 · 0.08	410	0.6 · 0.6 · 0.48
Bricks	Dune face	4.0	0.2 · 0.1 · 0.08	864	1.2 · 0.6 · 0.48
Tiles	Dune top	8.9	0.3 · 0.3 · 0.05	1,922	1.8 · 1.8 · 0.27

Table 2.1 Characteristics of structure elements used in the tests

In total, four tests were carried out, one test was performed for a collapsing dune foot revetment and three tests for a seawall with a low dun behind (Table 2.2). Regarding the dune foot revetment, this test is comparable with Test T01 of the earlier tests (WL | Delft Hydraulics, 2006b) where a revetment was absent and tests of WL | Delft Hydraulics (1987a), where the revetments were stable.

The effects of a vertical seawall as tested here, neither stable, collapsing or absent have not been studied yet. Therefore, three tests were carried out for this type of structure. The under water profile is equal to the under water profile of the dune foot revetment. However, the sloping dune face is replaced by a vertical wall. A horizontal part can be found landward of the wall at a (prototype) level of NAP +7 m. The most landward side of the profile is formed by a slope until a (prototype) level of NAP +15 m. Figure B.1 shows the outer geometry of the profile of the tests with a seawall.

Hard Structure	Dune foot revetment	Seawall
Stable	WL Delft Hydraulics (1987a)	T12
Collapsing	T11	T13
Absent	T01 (WL Delft Hydraulics, 2006b)	T14

Table 2.2 Overview of tests carried out

Similar to the set up of the model for Test T01 in WL | Delft Hydraulics (2006b), a depth scale factor of $n_d = 6$ and a profile steepness factor of $S_0 = 2$ is applied for all tests, because those values lead to wave conditions that can be generated by the wave generator and to a reference profile that fits in the flume, see Figure B.1. The mean sand diameter was $D_{50} = 200 \mu\text{m}$, which corresponds with an estimated fall velocity of $w = 0.023 \text{ m/s}$. This leads to steepness factors of $S_l = 1.52$ and $S = 1.32$. If the scale relations Equations 2.1 and 2.3 are correct, the outer geometry of the profile in the model corresponds to a prototype profile that is a factor 1.32 steeper than the reference profile.

Test T11 (collapsing dune foot revetment)

In Test T11, a revetment was applied on a dune with an outer geometry that was equal to Test T01 of the earlier tests (WL | Delft Hydraulics, 2006b). The revetment on the dune face

is constructed to a (prototype) depth of NAP +1 m. The lower part of the revetment is covered with sediment (from NAP +1 m to NAP +3 m in prototype). The revetment on the dune face mainly consists of the block elements (see Table 2.1). Also two rows of the brick elements are applied on the dune face. The elements are applied in colour bands, see Figure B.2 and Photo C.1: the lowest band of elements is grey, on top of that is a purple band, then a black one, a yellow one and the highest colour band on the dune face is red. The dune top is entirely covered with the tile elements that are also applied in colour bands: from the most seaward side of the dune top towards the landward side the colour bands grey, red and black are repeated in that order.

Test T12 (stable seawall)

The vertical wall is constructed of wooden beams to a (prototype) depth of NAP -8 m and is fixed to the flume walls to prevent it from collapsing during the wave attack. The top part of the profile is entirely paved with the tile elements (see Table 2.1) in colour bands, see Figure B.2 and Photo C.2. A geotextile is applied behind the vertical wall and underneath the elements. The geotextile has apertures with sizes of $O_{90} = 180 \mu\text{m}$ and weighs 235 g/m^2 . For cyclic flow the apertures should be about $O_{90} = 0.5 \cdot D_{90}$ to $O_{90} = 1 \cdot D_{90}$ (depending on the permissibility of sediment loss) in which D_{90} (m) is a measure for the size of the sediment.

Test T13 (collapsing seawall)

The vertical wall is constructed with the block elements (see Table 2.1) in colour bands to a (prototype) depth of NAP +1 m. The top part of the profile is entirely paved with the tile elements in colour bands, see Figure B.2 and Photo C.3. Since the revetment is assumed to collapse under extreme wave attack, the revetment is constructed with very few stability improving measures (no geotextile or cement).

Test T14 (absent seawall)

The dune (or the part of the profile above the still water level) is entirely made of sediment, see Photo C.4. Photo C.4 shows both the dune profile during construction and the profile just before the test. It should be noted that the last photograph was taken after the first profile measurement; the vertical part of the dune already shows some small collapses on the photograph, while these have not been measured.

2.3 Test conditions

Table 2.3 shows the test programme with the prototype and model values of the *desired* hydraulic conditions with the wave height H_{m0} , the wave periods T_p and $T_{m-1,0}$ and the wave steepnesses s_p and $s_{m-1,0}$. The hydraulic conditions in Tests T11, T12, T13 and T14 correspond with the conditions applied in Test T01 of the earlier series of dune erosion tests (WL | Delft Hydraulics, 2006b).

Test	Prototype			Model				
	H_{m0} (m)	T_p (s)	$T_{m-1,0}$ (s)	H_{m0} (m)	T_p (s)	$T_{m-1,0}$ (s)	s_p (-)	$s_{m-1,0}$ (-)
T11 –T14	9.0	12.0	10.9	1.5	4.90	4.45	0.040	0.049

Table 2.3 Test conditions with generated hydraulic conditions at wave board ($T_{m-1,0} = T_p / 1.1$)

A Pierson-Moskowitz wave spectrum was applied in each test. The spectral wave period $T_{m-1,0}$ in Table 2.3 is determined with the ratio of $T_p / T_{m-1,0} = 1.1$. For a standard single-peaked wave energy spectrum, such as the Pierson-Moskowitz spectrum, at deep water (near the wave board) this ratio comes close to a value of $T_p / T_{m-1,0} = 1.1$. Here, also the wave period $T_{m-1,0}$ is used, because for several coastal processes it has been found that this spectral wave period is a better characteristic wave period than the peak wave period (see WL | Delft Hydraulics, 1999; Van Gent, 2001; Van Gent *et al.*, 2003).

All tests were carried out with a water depth of 4.5 m in the flume near the wave board. A water depth of 4.5 m corresponds with a water depth of 27 m in prototype. With a storm surge level of NAP +5 m, this results in a bed level of NAP -22 m near the wave board.

The wave gauges used to measure the wave conditions had to be installed at some distance (approximately 1 wavelength) from the wave board. Since the water depth at the location of these wave gauges is different from the water depth near the wave board (see Figure B.1) the wave height at the measurement location also deviates somewhat from the wave height at the wave board.

The total duration of the tests was 6 hours. After the following fixed time intervals Tests T11, T13 and T14 (in which the revetments and/or dunes collapsed) were temporarily interrupted to carry out bed profile measurements:

- A. 0 till 6 minutes or 0 till 0.1 hour;
- B. 6 till 18 minutes or 0.1 till 0.3 hour;
- C. 18 till 60 minutes or 0.3 till 1.0 hour;
- D. 60 till 122 minutes or 1.0 till 2.04 hours;
- E. 122 till 240 minutes or 2.04 till 6.0 hours.

The time intervals in the beginning of the test are the shortest, because in the beginning of a test the erosion rates are the highest. Similar time intervals were used in earlier research (WL | Delft Hydraulics, 2006b). Time interval D was chosen to end after 2.04 hours, because 2.04 hours in the model corresponds to 5.0 hours in prototype at a depth scale of $n_d = 6$. The dune erosion rate after 5 hours in prototype at maximum storm surge level is found to be almost equivalent to the dune erosion rate due to a real storm event with a duration of more than 5 hours, but with a (more realistic) water level fluctuation with the same maximum water level. In the following chapters the characters A to E are sometimes added to the test name to indicate the time interval in which a measurement was carried out.

Test T12 in which the depth of the scour hole seaward of the revetment was investigated was interrupted at the following times to carry out profile measurements:

- B. 0 till 16.5 minutes or 0 till 0.3 hour;
- C. 16.5 till 60 minutes or 0.3 till 1.0 hour;
- D. 60 till 122 minutes or 1.0 till 2.04 hours;
- E. 122 till 240 minutes or 2.04 till 6.0 hours.

2.4 Measurements

The measurements carried out during the tests and the measurement devices used for this purpose are described in this section. Next to the measurements described hereafter also visual observations were carried out during the tests, which were supported with digital photographs and video recordings.

2.4.1 Bed profile

Mechanical profile follower and echo sounder

Since the measurement carriage on which the profile measurement devices are installed is too long to measure the profile near the wave board and the entire dune top with one device, both a so-called mechanical (amphibious) profile follower and an echo sounder are installed to measure the entire profile. The profile measurements are carried out before and after each test and after each temporary test interruption in three cross-shore transects (always with water in the flume): one along the longitudinal flume axis and the other two at 1.25 m on both sides of the flume axis. The profile measurement with the echo sounder is carried out only in the middle transect. The driving direction of the carriage is from the dune top to the wave board.

The measurement carriage drives over the rails on top of the walls of the flume with a maximum velocity of 0.15 m/s while the profile follower is moving over the bed. If the bed profile (or revetment) becomes steep (near-vertical) and the carriage drives with a high velocity, the wheel loses its contact with the profile around the steep part and therewith ‘misses’ that part of the profile. This loss of profile information is minimised by reducing the driving velocity to about 0.05 m/s around the steep parts of the profile. A sample frequency of 30 Hz is applied and the samples are horizontally interpolated to steps with a length of 0.01 m. The profile follower has a wheel with a diameter of 0.1 m and a width of 0.05 m, which is sufficiently accurate to follow the bed ripples. The diameter of 0.1 m also appeared to be sufficiently large to drive over the structure elements that were spread over the beach after the revetments collapsed. A photograph of the profile follower can be found in Appendix C (Photo C.5). At 224.54 m from the wave board a calibration beam is fixed over the entire width of the flume such that the top side of the beam is located at a distance of 6.17 m from the flume bottom. Before starting a profile measurement the profile follower is put on that beam to calibrate it. With the profile follower the part of the profile between 27 m and 225 m from the wave board was measured before and after each test and in most test interruptions. In some interruptions however, a smaller distance was measured, see Table A.1.

The measurement carriage also drives with a maximum velocity of 0.15 m/s while measuring with the echo sounder the part of the profile from 14 m to 27 m from the wave board. This is done before and after each test and in most test interruptions, see Table A.1. A sample frequency of 10 Hz is applied and the samples are horizontally interpolated to steps with a length of 0.01 m. The echo sounder transmits sound pulses that reflect on the bed returning to its source as an echo. The time interval between the initiation of a sound pulse and echo returned from the bed can be used to determine the depth of the bottom. At 13 m from the wave board a horizontal plate is fixed to the bottom of the flume such that the top side of the plate is located at a distance of 0.04 m from the flume bottom. Before starting a profile measurement the echo sounder is put above that plate for calibration.

If in the following chapters the average profile measurement is mentioned, it concerns the average of the three parallel measurements with the mechanical profile follower. In the averaging procedure each of the three measurements counts equally, thus no weight factors are applied to the measurements unless specifically mentioned. The average profile measurement does not give reliable information on profile features that vary strongly in cross-flume direction (*e.g.* bed ripples and structure elements). The transition between the average profile measured by the profile follower and the profile measured by the echo sounder might show a discontinuity, because of cross-flume irregularities in the profile.

Stereo video

Two cameras were used to obtain stereo video measurements. Stereo video requires at least two cameras looking at the same area in order to obtain 3D information on the water surface and bed profile from the video measurements. More information on stereogrammetry can be found in Holland and Holman (1997).

The two cameras are fixed to the shed roof above the flume axis at respectively 190.4 m (CAM1) and 196.8 m (CAM2) from the wave board at a height of 8.5 m. The cameras are pointed towards the inner surf and swash zone and to the dune face. They cover an area in the flume with a length of approximately 15 m and a width of approximately 5 m (see Photo C.6). The (synchronised) cameras take pictures at a frequency of 4 Hz. The times at which the pictures are taken can be related to the other measurements in the flume: the moment the recording of the other measurements starts a red LED (Light Emitting Diode) is turned on which is visible at pictures by CAM2 (see Photo C.7).

Use is made of the following cameras:

- Point Grey Scorpion 14SO cameras,
- Sony 1/2" ICX267 Progressive Scan CCD,
- 1392x1060 pixels, 8-bit monochrome with Bayer filter,
- First-order bilinear debayering to 24-bit RGB and JPEG (quality 80) compression.

Holland *et al.* (1997) describe the calibration technique for cameras for this purpose.

The technique to obtain bed profile information from the video measurements is still under development. The video data will be used in the analyses that contribute to this development.

2.4.2 Wave conditions and water depth

The wave heights and wave periods were measured during each test. The incident wave conditions were measured close to the wave generator. In addition, wave conditions were measured at several points along the profile.

The incident wave signal is determined with the measurements of two different (combinations of) instruments (see also Figure B.1):

- Three resistance-type wave height meters: WHM01, WHM02 and WHM03 (see Figure B.1). These devices measure the resistance of a wire that is installed vertically in the water over almost the entire water depth. The change in resistance can be translated to a change in water level and ultimately in a wave signal. By combining the measurements of the three wave height meters, the incident wave conditions are determined using the method of Mansard and Funke (1980). With this method the measured wave signal is corrected for the effect of reflected waves. The middle of the three meters is installed at a distance of 41 m from the wave board. The location of these wave height meters has been assessed on the basis of the requirement that the incident wave height should be measured at a distance of at least one wavelength (approximately) from the wave board. A sample frequency of 25 Hz is applied.
- One pressure sensor and one flow velocity meter: PS01 and EMS1 respectively (see also Figure B.1). With a pressure sensor (type Kulite HKM-375M-1) the water surface is measured. The pressure sensor is installed at 3.0 m from the bottom of the flume at a distance of 41 m of the wave board. In combination with a flow velocity meter installed at the same distance from the wave board just beneath the pressure sensor (at 2.75 m from the flume bottom) the incident wave signal (corrected for the effect of reflected waves) is determined. A method which has been used successfully in the field was presented by Guza *et al.* (1984). They used information from a co-located pressure sensor and a velocity meter and shallow water theory to separate shoreward and seaward propagating long waves. This is extended to linear wave theory. A sample frequency of 25 Hz is applied.

In addition, waves were also measured with pressure sensors (type Kulite HKM-375M-1) at 9 locations along the profile, see Table 2.4 and Figure B.1, identical to those in earlier tests, see WL | Delft Hydraulics (2006b). The measurements in these 9 locations give an

indication of the wave conditions along the profile, using a method that was explained a.o. by Dean and Dalrymple (1991).

As mentioned above, the location for measuring the incident wave height was determined on the basis of the requirement that it should not be within a distance of approximately one wavelength from the wave board. This resulted in a distance of 41 m from the wave board. The water depth at this location is different from the water depth near the wave board, see Figure B.1. Therefore, the wave height at this measurement location may also differ from the wave height at the wave board, due to wave breaking and shoaling.

Pressure sensor	Distance from wave board (m)	Distance from flume bottom (m)
PS01	41	3.00
PS02	70	3.00
PS03	100	3.40
PS04	130	3.40
PS05	150	3.40
PS06	170	3.40
PS07	190	3.95
PS08	200	4.15
PS09	205	4.30

Table 2.4 Positions of pressure sensors

A transition slope has been applied in the profile since the waves have to be generated at relatively deep water (in this case at a location where the bed level is at NAP -22 m in prototype), while the length of the flume is not long enough to construct the entire profile to this depth with the desired slope. In order to estimate the effects of this transition slope wave propagation computations with and without the transition slope have been made and computed wave heights just landward of the transition have been compared. The computations with TRITON (*i.e.* the time-domain Boussinesq-type wave model of WL | Delft Hydraulics, Borsboom *et al.*, 2000, 2001, and Van Gent and Doorn, 2001) indicate that the influence of a transition slope compared to a more realistic gentle foreshore slope towards deeper water is rather small. A more gentle slope instead of a steep transition slope may lead to wave heights that could be approximately 5% lower. For longer wave periods this difference is smaller.

The water depth is kept constant during the test series and it is checked before each test interval.

2.4.3 Other measurements

The water temperature is monitored in each test interval with a temperature sensor at about 180 m from the wave board.

The dimensions and masses of the different elements were measured above (see Table 2.1) and in water to obtain the densities of the different elements, see Table A.9.

Some characteristics of the sediment were measured in the dune erosion tests prior to the present tests, see WL | Delft Hydraulics (2006b). A large number of samples of the sediment (from the bed) were used to determine the particle size distribution by means of sieving from which the grain sizes D_{10} , D_{50} and D_{90} could be obtained. The mean and the standard deviation of the grain size D_{50} are 200 μm and 15 μm respectively.

The fall velocity of the sediment was also measured in the previous tests (WL | Delft Hydraulics, 2006b) with subsamples of the bed samples used for the determination of the particle size distribution. The temperature of the water of the settling velocity tests is measured, because it affects the velocity. Use is made of the VAT-method ('Visual Accumulation Tube') described in Van Rijn (1993). The inaccuracy of the fall velocity distribution determined with the VAT-method is about 10 % for particles with a diameter ranging from 50 to 500 μm . Based on these measurements it was concluded that the fall velocity could be estimated with the following relation:

$$\log(1/w) = a \cdot (\log D)^2 + b \cdot \log D + c \quad 2.7$$

where w (m/s) is the fall velocity, D (m) is the sediment diameter and a , b , and c are coefficients depending on the water temperature. For fresh water with a temperature of 10 °C they are 0.476, 2.180 and 3.190 respectively, and for water with a temperature of 18 °C they are 0.495, 2.410 and 3.740 respectively. For other water temperatures the values of the coefficients can be obtained by linear inter- or extrapolation.

The actual fall velocity of the sediment in the tests depends on the measured water temperature.

3 Results of physical model tests

3.1 Introduction

In this chapter the results of the tests are described. Further interpretations of the results can be found in Chapter 4.

Section 3.2 describes the results of the measurements of the wave conditions. Section 3.3 describes the profile development and erosion volumes based on these profile data. The results of other measurements are presented in Section 3.4.

All values presented in this chapter are ‘model values’ (viz. measures of and results of measurements in the physical model in the Delta flume), unless they are specifically referred to as ‘prototype values’ (corresponding to a field situation).

3.2 Wave conditions and water depth

The wave conditions were measured continuously during all test intervals. The time intervals D and E provide the best realisation of the desired wave spectrum, because they are sufficiently long (> 500 waves).

Table A.2 shows the incident wave conditions measured with the wave height meters WHM01, WHM02 and WHM03. The signals of the three wave height meters are combined to derive the incoming waves (propagating in the direction from the wave board to the dune face) by excluding the reflected waves with the method of Mansard and Funke (1980). Figure B.10 to Figure B.13 show the wave height exceedance curves and energy density spectra of the incoming (without the reflected) waves in Tests T11E, T12E, T13E and T14E respectively (Test T11E corresponds with time interval E in Test T11, see Section 2.3). The reflection coefficients were 0.23, 0.22 and 0.23 for Tests T11E, T13E and T14E respectively. In Test T12, where the vertical seawall was stable, the reflection coefficient was 0.27 in interval A, at the start of the test, while in interval E, at the end of the test, the coefficient was 0.30. This increase in reflections was also visually observed.

The individual measurements of the three wave height meters can be found in Table A.3. During the time interval B, C and E in Test T12 the wave machine was stopped at one moment in time to inspect the structure. The measurements before and after these failures were combined for the analyses.

Table A.4 shows the incident wave conditions measured with pressure sensor PS01 (at a distance of 41 m from the wave board) and flow velocity meter EMS01 (at the same distance from the wave board). The positions of these instruments can be found in Figure B.1. From a comparison of the incident wave conditions presented in Table A.2 (based on resistance type gauges) it can be concluded that the wave heights H_{m0} as assessed for the intervals D and E are similar for both methods (based either on wave height meters or based

on the pressure sensor in combination with the velocity meter). The maximum deviation in the wave height between two simultaneous measurements with the different methods was found in Test T12 and is 0.07 m, which is approximately 5 % of the measured value. Also the obtained values for the peak wave period are similar for the test intervals D and E. The maximum deviation in the peak wave period between two simultaneous measurements is 0.1 s, which is approximately 2 % of the measured value, and the differences between the 2 methods for the spectral wave period $T_{m-1,0}$ is 0.2 s, which is approximately 4 %.

At the wave board the wave height was for all tests $H_{m0} = 1.5$ m and the peak wave period $T_p = 4.9$ s. The software to generate wave steering signals for the Delta flume is called Delft-AUKE/generate and has been tested in a number of flumes and basins, including WL | Delft Hydraulics' Delta flume. In general, the target wave conditions are generated with an error of less than 5% (in terms of significant wave height) in the first attempt.

Table A.5, Table A.6 and Table A.7 show the wave conditions derived with the measurements with pressure sensors PS01 to PS09. It is not possible to make a distinction between incoming and reflected waves using a single pressure sensor at a certain location. The applied method to obtain estimates of the wave height also makes use of the water depth at the location of the measurement which varies at some locations. Use is made of the average depth based on the profile measurements before and after a test interval.

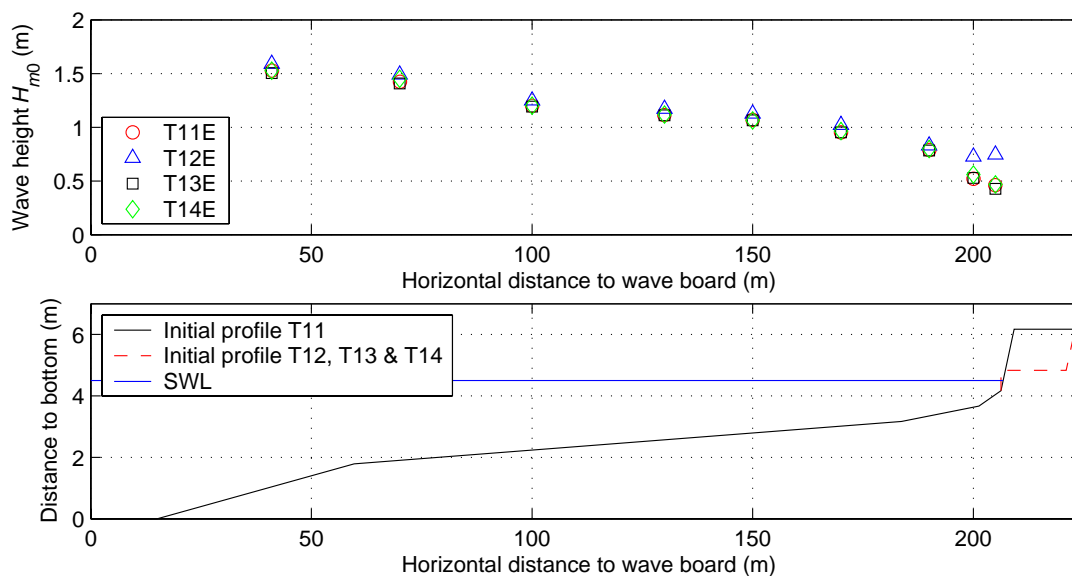


Figure 3.1 Wave heights over coastal profile from pressure measurements

Figure 3.1 shows the wave heights over the coastal profile obtained from the measurements with the pressure sensors. The differences in wave heights in the different tests until 190 m from the wave board are relatively small. In the two sensors closest to the dune (at 200 m and 205 m from the wave board), the wave height in Test T12 is larger than in the other tests. The water depth at those locations in Tests T11, T13 and T14 decreases with the increase of the volume of eroded sediment, which causes more wave breaking and reduces the wave height. In Test T12 there is a scour hole in front of the seawall that leads to a larger wave height.

Figure B.14 shows the energy density spectra obtained from the measurements with the pressure sensors in each test. These graphs show that the energy density in the peaks decreases rapidly while the waves propagate along the profile in landward direction and that the contribution of energy in lower frequencies becomes larger. The energy density spectra are almost equal in each test. The differences between Test T12 on the one hand and Tests T11, T13 and T14 on the other hand are the largest at 200 m and 205 m from the wave board.

During the tests it was observed that the pressure sensor closest to the dune (PS09) sometimes was above the water level. The water surface elevations obtained from that pressure sensor are not corrected for the periods of time in which it was above the water level.

3.3 Profile changes and dune erosion volumes

In this section the bed profile changes from visual observations and from bed profile soundings during and after the tests are described. Use is sometimes made of the average of the three profiles measured with the mechanical profile follower (see Section 2.4.1). In the averaging procedure each of the three measurements counts equally, thus no weight factors are applied to the profile data unless specifically mentioned otherwise. The average profile measurement does not give reliable information on profile features that vary strongly in cross-flume direction (*e.g.* bed ripples and structure elements).

3.3.1 Test T11: reference dune profile with revetment

Visual observations on erosion process

Wave run up is frequently observed over the dune face onto the dune top, see Photo C.8. Nevertheless, during Test T11A the revetment remained entirely intact (Test T11A corresponds with time interval A in Test T11, see Section 2.3). No significant displacements of stones could be visually observed.

After about 9 minutes in Test T11 a couple of elements in the purple colour band on the top-third row on the left side of the flume start to show some settlement. A sediment-water mixture starts washing out during the down rush of the waves at that location. After about 15 minutes sediment washes out at multiple locations, but most significantly noticeable at the purple colour band in the middle of the flume, see Photo C.8. Also a row of black elements settles on the left side of the flume. A small gap is present at the intersection of the dune face and the top of the dune at the end of this test interval.

After 20 minutes in Test T11 a row of black elements on the top side of the colour band shows significant settlement. After 21 minutes one of the rows with the yellow elements starts to settle. The number of locations where the sediment-water mixture washes out the revetment increases as well as the intensity of the washing out. After about 21.5 minutes both rows of yellow elements show significant settlement, see Photo C.9. After 23 minutes the first red elements move out of the revetment in the middle top part of the dune face, see

Photo C.9. After about 26 minutes the first grey elements of the revetment on the dune top move out of the structure start to displace and slide down the dune face. Soon thereafter almost all red elements are displaced from their original location. A large part moved down the dune face. The rows of black and the yellow elements are significantly settled, but still more or less in place. The settlement and the tight placement of these elements cause some rows of elements to form an arch between both flume walls therewith increasing their resistance from displacement out of the revetment. This situation remains unchanged until about 31 minutes after the start of the test when also the yellow elements start to displace, followed by the black elements after about 33 minutes. After about 35 minutes the purple elements start to displace. After about 43 minutes the entire revetment on the dune face is damaged above the grey colour band of which the top side is located around the still water level. This moment can be considered to be the moment of failure of the revetment, because the elements on top of the dune do not contribute to the 'strength' of the dune as a whole. About 1.5 rows of the grey elements on the dune top are displaced over the dune face towards the toe of the structure.

A scour hole develops seaward of the revetment (which is further described in the section on cross-shore bed profile measurements), but it cannot be observed whether the lowest part of the revetment on the dune face collapsed because of this scour hole or if it is still intact after Test T11C.

After the failure of the revetment (during Test T11D and T11E) the erosion process is similar to the erosion process of a dune without a revetment described in WL | Delft Hydraulics (2006b). When a lump of sediment falls down the dune face, a row of structure elements falls down with it. The elements that fall down from the dune top and the small elements of the (remains of the) revetment on the dune face are separated by a more or less 'clean' beach of about 1 m, see Photo C.10 and Photo C.11. During Test T11E the distance between the dune face and the elements that fall down from the dune top grows to about 1 m. Effects of the structure elements on the beach and the remaining elements on the dune top and at the toe of the revetment on the erosion process could not be observed visually.

In summary, the strength of the undamaged revetment decreases rapidly when individual elements or rows of elements start to settle and displace. The settlement and displacement is caused by the loss of sediment underneath the revetment through the elements. This can be seen as the failure mechanism of this revetment. At some moments in the test some irregularities were observed in cross-flume direction, but in general the process can be considered to be fairly two-dimensional.

Visual observations on post-test profiles

The bed surface was inspected after the water was pumped out of the flume. The surface of the profile generally was very smooth and no bed ripples were observed. Three grey elements of the dune top could be observed on the toe of the revetment on the dune face, see Photo C.11, together with a number of red and purple elements from the dune face. One grey element of the dune top could be found at about 2 m from the toe of the revetment on the bed. Not more elements could be found on top of the bed. The majority of the elements could be retrieved underneath the bed at the toe of the revetment. A scour hole developed at that location during the first part of test in which the elements that moved out of the

revetment landed and were buried by the eroded sediment. Two black, five red and five purple elements of the dune face and three grey elements from the dune top could be found just beneath the bed level at around 198 m from the wave board. The lowest part of the revetment on the dune face (which was located around 0.5 m underneath the bed level) appeared to be still intact. Apparently, not much elements were displaced much more seaward than the initial location of the revetment.

A cross-flume curvature was observed in the bed profile from about 60 m from the wave board to about 200 m. The top of the curvature was located in the middle of the flume and the lower parts next to the flume wall. This was also observed in the previous dune erosion tests (WL | Delft Hydraulics, 2006b) and in earlier research (WL | Delft Hydraulics, 1995). It is not exactly known why this curvature develops. It might be reasoned that it affects the water movement in the flume. Since the relative changes of the bed level are so small, it is assumed that the effects of the cross-flume curvature on the dune erosion process and on the dune erosion volumes above the still water level are negligible. However, it should be taken into account when the conservation of volume of sediment over the entire flume is analysed.

Cross-shore bed profile measurements

Figure B.3 shows the time-development of the average of the measured cross-shore profiles for Test T11. The figure shows that until 0.3 hour a scour hole develops seaward of the revetment until the lowest level of the revetment. It is possible that the maximum depth of the scour hole is deeper than that, but the next profile measurement (after 1 hour) took place after the revetment collapsed and the sediment and elements that became available after the collapse probably filled the scour hole. The irregularities in the bed profile just above the still water level are caused by the structure elements. The wheel of the amphibious profile follower appeared to be large enough to drive over the structure elements. The structure elements on the beach might influence the (accuracy of the) calculation of the conservation of volume of sediment based on the profile measurements, because they are not evenly distributed over the width of the flume. The wheel of the profile follower might have driven just in between the elements or just over the largest pile of elements.

Figure B.4 shows that after the collapse of the revetment the development of the bed profile becomes similar to the profile development in a situation without revetment. Test T01 of the earlier dune erosion tests (WL | Delft Hydraulics, 2006b) is used for the situation without revetment, because this test was carried out with equal hydraulic conditions and an equal initial profile (outer geometry):

- The dune face shows a retreat which is clearly non-linear in time;
- The eroded sediment deposits in the area in front of the dune;
- The seaward edge of the deposit area becomes more clearly visible after 2.04 hours and after 6 hours test duration;
- The profile only shows a considerable development in a relatively small part of the entire profile in the flume between about 170 m and 215 m from the wave board. The rest of the profile does not significantly change during the tests.

Thus, the revetment on the dune face adds more to the strength, than the revetment on top. The differences between the following features of the profile in Tests T11 and T01 clearly become smaller towards the end of the test:

- In Test T01 the position (in a horizontal sense) of the **dune face** is located further landward at all times than in Test T11, but the distance decreases towards the end of the test;
- At the start of the test the differences are (obviously) very large, but especially after 6 hours the similarities in the **slope around the still water level** are striking;
- After 6 hours the location, but also the shape of the **seaward edge of the deposition area** are very much alike.

Figure 3.2 compares the retreat of the dune face in Tests T11 and T01. The horizontal distance between the initial position of the dune face and the measured position after a certain period of time at 5.5 m (corresponding to a level of NAP +11 m in prototype) from the flume bottom is used for this purpose. The dune face retreat is somewhat larger in Test T01 than in Test T11 at all times, but the difference is small. The effects of a revetment on the retreat of the dune face seem to be small; at least the revetment does not seem to increase the retreat of the dune face.

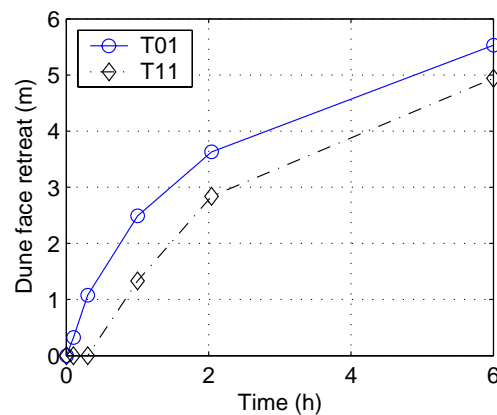


Figure 3.2 Development of retreat of dune face in time in Tests T01, and T11

In summary, the effects of a revetment on the profile development strongly depend on the moment the revetment collapses, or on the strength of the revetment. The differences in the profile development between Tests T11 and T01 are small. It is likely if Test T11 would have continued for 43 minutes more (or Test T01 for 43 minutes less), the difference between Tests T01 and T11 would have been even smaller. It can therewith be concluded that there are no important effects of a revetment at a dune with a geometry according to the reference profile on the profile development in the 2D situation.

Erosion volumes

Table 3.1 shows the dune erosion volumes above the still water level (or storm surge level), see Figure 1.2 for a graphical illustration of this erosion volume. The dune erosion volume is based on the difference between the initial profile and the profile measured after a certain

period of time. The table also shows the increase in erosion volume since the last profile measurement.

Time (h)	Erosion volume (m ³ /m ¹)		Increase in erosion volume (m ³ /m ¹)	
	T01	T11	T01	T11
0.0	0.00	0.00	0.00	0.00
0.1	0.90	0.00	0.90	0.00
0.3	2.13	0.00	1.23	0.00
1.0	4.23	2.35	2.10	2.35
2.04	5.88	4.61	1.65	2.26
6.0	8.60	7.82	2.72	3.21

Table 3.1 Dune erosion volumes above still water level and increase in erosion volumes in Tests T01 and T11

Table 3.1 also shows the erosion volumes obtained from Test T01 of the earlier tests (WL | Delft Hydraulics, 2006b) for the reference situation without revetment. Obviously, the erosion volumes in Test T01 are larger than the volumes in Test T11 at all times. However, the increase in erosion volume after a certain profile measurement compared to the previous profile measurement is larger in Test T11 at all times. If the moment at which the revetment entirely failed (after 25 minutes in Test T11C) is used as the start time for the erosion development, a slightly different development is obtained (represented with the blue dash-dot-line in Figure 3.3).

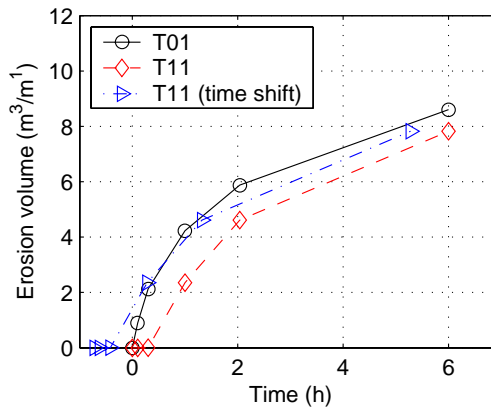


Figure 3.3 Development of erosion volume in time in Tests T01 and T11

The effects of this collapsed revetment on the development of the erosion volume in time are small. The effects of a revetment in the initial profile on the total dune erosion volume after 2.04 or 6 hours are also not very large compared to a situation without a revetment and would have been smaller if the revetment would have collapsed sooner. It is however (still) not very likely, that an instant collapse of the revetment at the start of the test would have led to a higher dune erosion volume than in a situation without a revetment. It can therewith

be concluded that there are no important effects of a revetment at a dune with a geometry according to the reference profile on the dune erosion volume in the 2D situation. The dune erosion volume does not increase because of these elements and does not significantly decrease either.

3.3.2 Test T12: scour hole at vertical wall

Visual observations on erosion process

The relative small freeboard of the revetment caused large overtopping discharges; water could be observed on the horizontal part of the revetment almost continuously, see Photo C.12.

During Test T12 the erosion took place entirely under the water surface. Direct visual observations on the dune erosion process could therefore not be made. However, towards the end of Test T12E larger wave reflections seemed to occur that could indicate an increased water depth in front of the vertical wall.

Towards the end of the test some sediment could be found on the dune top around 220 m from the wave board. Since the entire revetment is protected with a geotextile, this sediment is expected to originate seaward from the revetment and transported by the overtopping waves.

The bed surface was inspected after the water was pumped out of the flume. The surface of the bed profile including the area around the scour hole generally was very smooth and no bed ripples were observed, see Photo C.13. After Test T12 a cross-flume curvature could be observed (like after Test T11). However, around the scour hole the cross-flume bed profiles were fairly horizontal.

Cross-shore bed profile measurements

After the first couple of minutes of the test the vertical wall needed to be reinforced with a beam of steel (installed on top of the wall, see Photo C.13). Therefore, the initial profile measurement deviated slightly from the measurements thereafter at that location. To facilitate the analyses of the profile data, the data from the initial profile measurement is replaced with the data of the subsequent profile measurement around the vertical wall.

Figure B.5 shows the time-development of the average of the measured cross-shore profiles for Test T12. Already after 0.3 hour, a scour hole is clearly present. In time, the scour hole increases in size, but more in longitudinal direction than in depth (see also Figure 3.4). The angle at which the profile connects to the revetment becomes less steep during the test. The top of the accretion area moves in seaward direction towards the end of the test.

Table 3.2 and Figure 3.4 show the volume of the scour hole and the maximum depth of the scour hole (defined as the vertical distance of the initial bed level to the bed level at the deepest part of the scour hole). The volume increases almost linearly in time, especially after 0.3 hour, whereas the scour depth only shows a very small increase after 0.3 hour.

The initial water depth at the location of the maximum depth of the scour hole was $h_i = 0.33$ m. At the end of the test, the maximum depth of the scour hole is almost 2 times the initial water depth.

Time (h)	Volume of scour hole (m ³ /m1)	Max. scour depth $d_{s,max}$ (m)	Min. breaker depth h_b (m)	Initial water depth h_i (m)	Rel. depth $d_{s,max} / h_i$ (-)	Rel. depth $(d_{s,max} + h_i) / h_b$ (-)
0.0	0.0	0.0	0.0	0.33	0.0	0.0
0.3	0.28	0.44	0.48	0.33	1.3	1.6
1.0	0.43	0.56	0.57	0.33	1.7	1.6
2.04	0.65	0.58	0.66	0.33	1.8	1.4
6.0	1.30	0.63	0.69	0.33	1.9	1.4

Table 3.2 Volume and maximum depth of scour hole in Test T12

Figure 3.4 also shows that the minimum water depth on the bar (h_b) develops more or less in the same fashion as the maximum scour depth. Further interpretations on the scour hole including a comparison with results from previous investigations can be found in Chapter 4. In earlier tests with sloping revetments it was found that the steeper the revetment the closer the location of maximum scour depth to the revetment. This is in agreement with Test T12, because the location of maximum scour depth can be found directly next to the revetment at all times in Test T12. It was also found in the earlier tests that the steeper the revetment the faster the development of the scour hole towards an equilibrium depth. This is confirmed with the results of Test T12. The scour depth in Test T12 relative to the initial water depth ($d_{s,max} / h_i \approx 2$) seems to be somewhat larger than in the earlier tests.

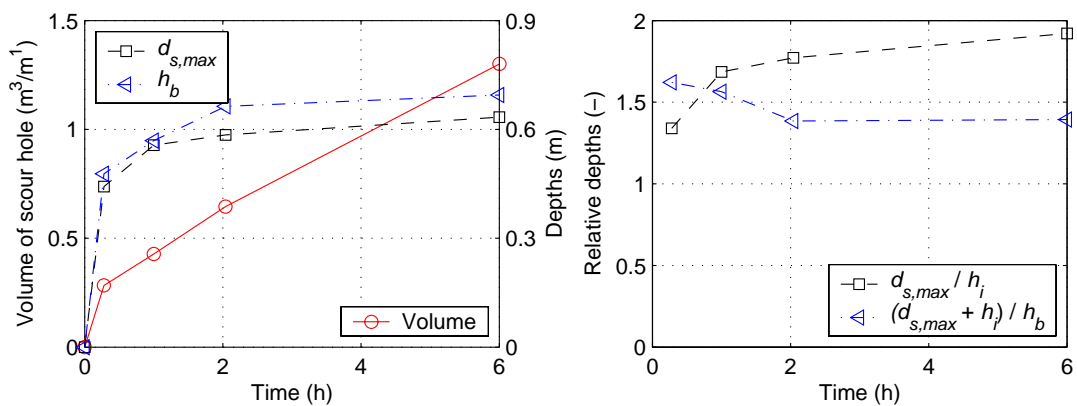


Figure 3.4 Development of volume and of maximum depth of scour hole in time in Test T12

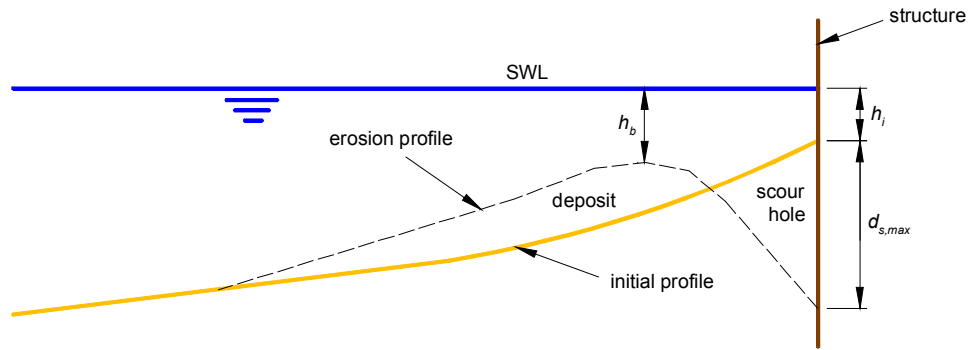


Figure 3.5 Definition sketch of scour hole

3.3.3 Test T13: relatively low dune with revetment

Visual observations on erosion process

Already with the first couple of waves the vertical part of the revetment collapsed, see Photo C.14. The small black elements moved up the horizontal part of the revetment; the yellow elements moved under water. The sediment of the dune and the large elements of the horizontal part of the revetment eroded very rapidly. Some large elements were displaced seaward, but most in landward direction.

Wave overtopping was frequently observed during the entire test. The overtopping waves moved both sediment and structure elements landward. During Test T13D the connection between the undamaged (initial) profile and the eroded profile above the water level became rather smooth, see Photo C.15. In fact, the eroded profile continued more or less on top of the undamaged profile, because of all the sediment and elements that were transported to that location. A near vertical profile between a beach and the top of the dune was no longer present. The erosion process seemed to progress slower from that moment on.

Visual observations on post-test profiles

The bed surface was inspected after the water was pumped out of the flume. The surface of the profile generally was very smooth and no bed ripples were observed, except around 75 m from the wave board. At that location a series of similarly shaped holes could be observed of about 25 cm deep and about 1 m long (in cross-shore direction), see Photo C.16. The holes can also be discerned in the profile measurements, see Figure B.6.

It is not entirely clear why these holes developed in this test. Only some small fluctuations in the bed level at about the same location were observed after Test T11, but after Test T12 no fluctuations were found at all. The series of holes can also be characterised as large bed-ripples. Ribberink and Al-Salem (1994) found ripples with about the same size in a wave tunnel for a regular oscillatory flow. However, ripples were not observed for irregular and asymmetric flow. It was reasoned that the development of these ripples is very sensitive for the conditions in the experiments (e.g. sediment characteristics and hydraulic conditions).

In Test T13 a very specific combination of hydraulic conditions and sediment characteristics might have occurred that created these ripples. The shape of the initial profile might however also have contributed to the formation of these holes. Maybe they are just a model effect or a combination of the above mentioned possible causes. Since the holes are relatively far from the dune, they are expected not to affect the dune erosion process. Their origin and development are therewith less relevant to analyse further into detail for the purpose of dune erosion.

Photo C.16 shows that the lower (grey) part of the vertical revetment is almost entirely intact. Some of the elements that were displaced could be found just seaward of the vertical revetment on the bed. In the main deposition area in front of the vertical revetment (from 185 m to about 206 m from the wave board) some elements could be found somewhat buried in the sediment: around 198 m from the wave board 4 small (red) elements and 1 large (yellow) element were found and around 199.5 m from the wave board another 6 (4 red and 2 black) small elements were found. Apparently, not much elements were displaced much more seaward than the initial location of the revetment. In the other deposition area (at about 220 m from the wave board) 67 small (black) elements could be found of which most were buried in the sediment and under the larger elements.

After Test T13 a cross-flume curvature could be observed (like after Tests T11 and T12).

Cross-shore bed profile measurements

Figure B.6 shows the time-development of the average of the measured cross-shore profiles for Test T13. The figure shows that the retreat of the dune face is very fast in the beginning of the test and slows down towards the end. After 0.3 hour a dune face is still present, but in the profile measurements after 1 hour, 2.04 hour and 6 hours a dune face cannot clearly be observed: the beach slope continues over the undamaged part of the horizontal profile. After 6 hours the erosion profile almost reaches the sloping part of the revetment. The seaward edge of the deposit area becomes more clearly visible after 2.04 hours and after 6 hours. The profile only shows a considerable development in a relatively small part of the entire profile in the flume between about 170 m and 220 m from the wave board. The rest of the profile did not significantly change during the tests.

In the following section (Section 3.3.4) the results of the bed profile measurements in Test T13 are compared with the results of Test T14. The dune profile consisted solely of sediment (no revetment was constructed) in Test T14, and the hydraulic conditions and outer geometry of the dune profile were identical to those in Test T13.

Erosion volumes

Table 3.3 shows the erosion volume above the still water level (defined as A in Figure 1.2) and the total erosion volume ($A + A_2$ in Figure 1.2) in time for Test T13. Figure 3.6 shows the same (graphically). From this figure it becomes clear that the development of the erosion volume is still more or less logarithmic. For the erosion development in the previous tests with the reference profile as initial bed profile, this was already verified. Apparently, the shape of the initial profile and the presence of hard elements do not largely affect this behaviour. The erosion volumes in Test T13 are approximately a factor 2 smaller than the

tests with the reference profile as initial profile (e.g. Test T11 or Test T01 of the earlier dune erosion tests, see WL | Delft Hydraulics, 2006b), see Table 3.1.

Time (h)	Erosion volume above still water level (m^3/m^1)	Total erosion volume (m^3/m^1)
0.0	0.0	0.0
0.1	0.86	1.21
0.3	1.72	2.17
1.0	2.46	3.14
2.04	3.08	3.97
6.0	3.64	5.07

Table 3.3 Erosion volumes above still water level and total erosion volumes in Test T13

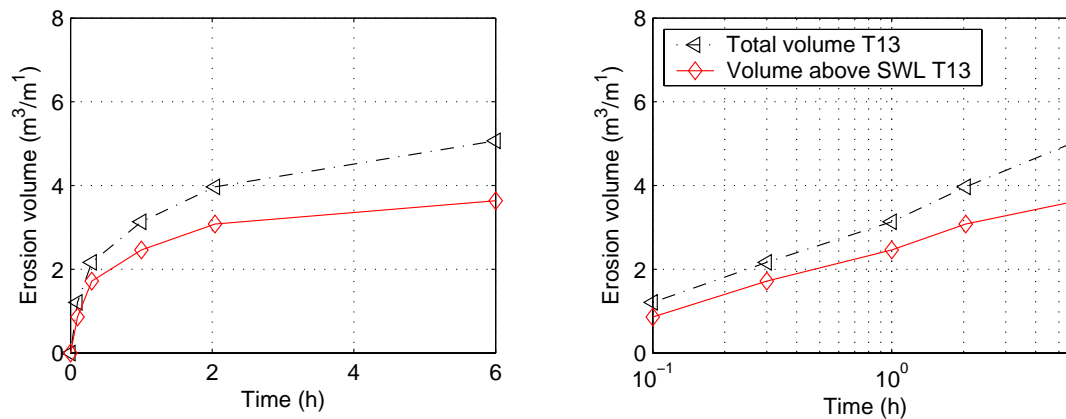


Figure 3.6 Development of erosion volumes in time in Test T13

3.3.4 Test T14: Test T13 without revetment

Visual observations on erosion process

The first waves already ‘washed over’ the vertical part of the dune profile. Both the wave impacts and the rundown of the waves on this vertical part caused a quick smoothing of the dune profile at that location during Test T14A, see Photo C.17.

The bed profile above the still water level transformed into a beach-like profile (with a gentle slope) soon thereafter. This beach stretched towards the steeper part of the profile at the back of the flume, see Photo C.18. Photo C.18 also shows some (very limited) erosion at the steeper part of the bed profile that is caused by a small number of waves that travelled over the entire beach up to that location.

Visual observations on post-test profiles

The bed surface was inspected after the water was pumped out of the flume. It was very similar to the bed surface after Test T13, where large bed ripples or holes were observed around 75 m from the wave board. These holes can also be discerned in the profile measurements, see Figure B.7. Some rather peculiarly shaped holes could also be observed between 120 m and 160 m from the wave board. Their depth was about 0.25 m and length (in along flume direction) 2 m to 5 m. They did not show the same periodicity as the ripples around 75 m from the wave board. Since also these holes are relatively far from the dune, they are expected not to affect the dune erosion process. Their origin and development are therewith less relevant to analyse further into detail for the purpose of dune erosion.

After Test T14 a cross-flume curvature could be observed (like after Tests T11, T12 and T13).

Cross-shore bed profile measurements

Figure B.7 shows the time-development of the average of the measured cross-shore profiles for Test T14. The figure shows that the retreat of the dune face is very fast in the beginning of the test and slows down towards the end. After 0.3 hour a dune face is still present, but in the profile measurements after 1 hour, 2.04 hour and 6 hours a dune face cannot clearly be observed: the beach slope extends to the steeper part at the back of the flume. Although a very small erosion area can be observed in that steeper part, some shoreward directed sediment transport must have taken place to create the deposit of sediment around 220 m. The seaward edge of the deposit area becomes more clearly visible after 2.04 hours and after 6 hours.

Figure 3.7 compares the retreat of the dune in Tests T13 and T14. The horizontal distance between Points P and Q (defined in Figure 1.2) is used for this purpose. It shows that the retreat is somewhat larger in Test T14 than in Test T13 at all times, but the difference is small. The effects of a revetment on the retreat of the dune seem to be small; at least the revetment does not seem to increase the retreat of the dune.

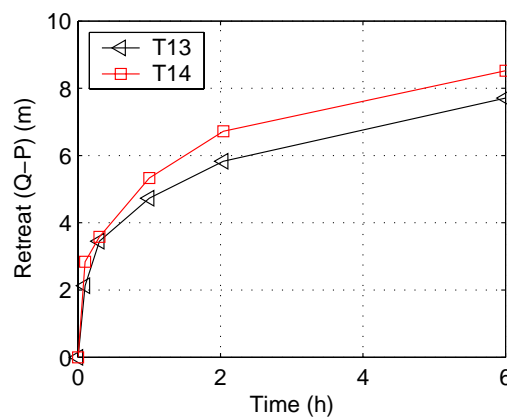


Figure 3.7 Development of retreat of dune in time in Tests T13 and T14

In Figure B.8 the profile development of Tests T14 and Test T13 (with revetment) are compared. Figure B.8 shows that the development of the bed profile around the vertical part of the dune is much faster in Test T14 than in Test T13. After 1.0 hour the vertical part is completely removed in Test T14 and transformed into a smooth beach slope, while in Test T13 some remains of the vertical part can still be clearly observed at that time. The shape of the bed profile under the still water level is very similar in both tests already after 1.0 hour. The slope of the bed profile around the still water level is almost equal after 2.04 hour. After 6.0 hours the entire bed profile is very much alike in both tests. Only at the steeper part of the profile some small differences exist. The beach is extended a little more landward in Test T14 than in Test T13, and the steeper part in Test T14 shows some small erosion, while no erosion can be observed in Test T13. The wave attack at that location is obviously very small. Apparently it is just large enough to cause some erosion in Test T14, but too small to cause damage to the revetment in Test T13 at that location.

Based on Figure B.8 it can be concluded that the effects of a revetment (of loosely packed relatively small elements) on dune erosion are very small, if the bed profile after 6.0 hours is considered. It can be seen that the initial profile development is somewhat slowed down by the collapsing revetment, but once the revetment has completely collapsed the bed profile rapidly develops to a bed profile that is very similar to a dune with the same outer geometry but without revetment.

Figure B.9 shows the profile development of Tests T14 and T01 of the earlier dune erosion tests (WL | Delft Hydraulics, 2006b) with equal hydraulic conditions. The profiles in this figure are horizontally translated such that the intersection of the still water level and the profile coincides in both tests. The bed profiles under the still water level after 2.04 hour are clearly different, see Figure B.9. The slope around the still water level is gentler in Test T14 than in Test T01 and the seaward edge of the deposition area is located further seaward from the intersection of the still water level and the bed profile. The shape of the seaward edge of the deposition area in Test T14 does show some agreement with the one in Test T01. Apparently, the shape of the initial profile somewhat affects the shape of the erosion profile (e.g. the slope of the erosion profile around and below the still water level). In the dune erosion prediction method by Vellinga (1986) the shape of the erosion profile solely depends on the hydraulic conditions and the fall velocity of the sediment. The influence of the initial profile on the erosion profile is not taken into account. It is recommended to further investigate the influence of the initial profile on dune erosion with dedicated physical model tests.

It is probable that the gentle initial profile of Test 14 is closer to the final equilibrium than the steeper initial profile of Test 01. In other words, it takes more time for Test 01 to reach the final state. This means that the duration of the storm also plays a role. It is therefore recommended to further investigate the role of the storm duration.

Erosion volumes

Figure 3.8 shows the erosion volume above the still water level (defined as A in Figure 1.2) and the total erosion volume ($A + A_2$ in Figure 1.2) in time for Test T14. From a comparison with the erosion volumes in Test T13, see Table 3.3, it can be concluded that the erosion volumes above the still water level in Tests T13 (with revetment) and T14 (without

revetment) are almost equal after 2.0 and 6.0 hours. The total erosion volume is somewhat larger in Test T14 than in Test T13. Figure 3.8 confirms these observations.

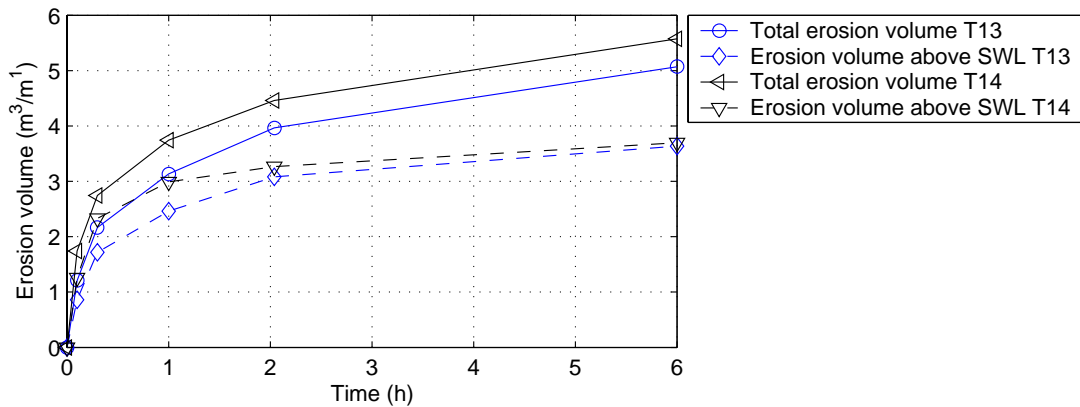


Figure 3.8 Development of erosion volumes in time in Tests T13 and T14

Figure 3.8 also shows that the erosion volume above the still water level develops faster in Test T14 than in Test T13 in the first hour of the test. After 2.04 hours (and still after 6.0 hours) however, the erosion volumes are almost equal in both tests. This was also concluded based on the profile development in Figure B.8. Apparently, the effects of a revetment (of loosely packed relatively small elements) on dune erosion are very small, if the erosion volumes above the still water level after 2.04 and 6.0 hours are considered.

Time (h)	Erosion volume above still water level (m³/m¹)	Total erosion volume (m³/m¹)
0.0	0.0	0.0
0.1	1.26	1.74
0.3	2.33	2.75
1.0	2.99	3.74
2.04	3.27	4.46
6.0	3.70	5.57

Table 3.4 Erosion volumes above still water level and total erosion volumes in Test T14

Figure 3.9 includes the development of the erosion volumes in Test T01 of the earlier dune erosion tests. This test was carried out with the same hydraulic conditions, but with the reference profile as initial profile and without revetment. The erosion volumes above the still water level in Test T14 are approximately a factor 2 smaller than the volumes in Test T01. Besides, the differences between total erosion volumes and erosion volumes above the still water level are much larger in Tests T13 and T14 than in Test T01. From Figure B.6 and Figure B.7 it becomes clear that a large part of the erosion takes place below the still water level.

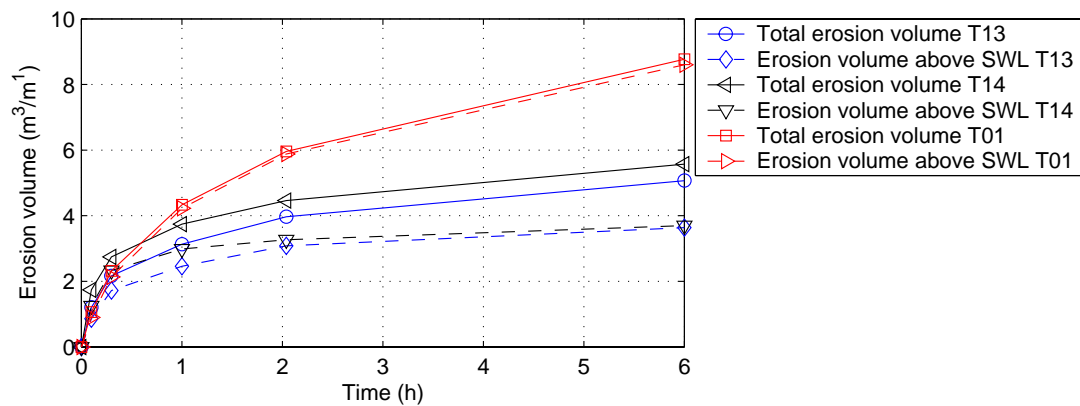


Figure 3.9 Development of erosion volumes in time in Tests T01, T13 and T14

3.4 Other measurements

Table A.8 shows the measured water temperatures. The temperature varied during the tests between 10.7 °C in Test T11C and 15.4 °C in Test T14. The average temperature was 10.9 °C, 13.9 °C, 13.3 °C and 15.2 °C for Tests T11, T12, T13 and T14 respectively.

Equation 2.7 can be used for estimating the fall velocities in combination with the coefficients depending on the water temperature. This results in a fall velocity of $w = w_{50} = 0.023$ m/s for Test T11 and for Tests T12, T13 and T14 in a fall velocity of $w_{50} = 0.024$ m/s, corresponding with the average grain size of $D = D_{50} = 200$ μm .

4 Further interpretations of results

4.1 Introduction

Further interpretations of the results presented in Chapter 3 are described in this chapter. The results of these interpretations are useful for further developments of the safety assessment methodology of dunes in The Netherlands, *e.g.* for the VTV for the period between 2006 and 2011.

4.2 Effects of hard elements in safety assessment

The VTV describes the procedure of assessing the safety of the Dutch dunes in ‘Katern 6’. In this procedure a distinction is made in two situations, a situation with a sandy dune without revetments, and a situation with a dune with a revetment, see Figure 6-4.2 in Ministry of Transport, Public Works and Water Management (2004). For the situation with revetment a reduction can be applied on the dune erosion calculated for the situation without revetment. This reduction depends on the level of the top side of the revetment and can only be applied if the revetment does not collapse under the normative storm conditions. “Katern 5”, “Katern 7” and “Katern 8” of the VTV (Ministry of Transport, Public Works and Water Management, 2004) provides the regulations to determine whether the revetment is stable. The reduction due to a stable dune foot revetment is described in Appendix VII of TAW (1995). The VTV recommends an advanced assessment by experts for other types of revetments.

If a revetment appears not to be stable under the normative storm conditions, the TAW (1995) prescribes that no reduction on the dune erosion due to the revetment can be taken into account. TAW (1995) even states that there is insufficient evidence to conclude that a collapsed revetment never leads to more dune erosion than a dune without revetment. Based on the results of Tests T11 and T13 (see Sections 3.3.1 and 3.3.3), it can now be concluded that there are no important effects of a revetment at a dune with a geometry according to the reference profile on dune erosion in a 2D situation. The dune erosion volume does not increase because of these elements and does not significantly decrease either. It seems legitimate to recommend the use of the standard safety assessment method for similar situations, therewith neglecting the presence of a revetment. Since this applies only for revetments that collapse soon after the start of extreme storm conditions, it is very important to know whether the revetment itself is stable or not under these conditions.

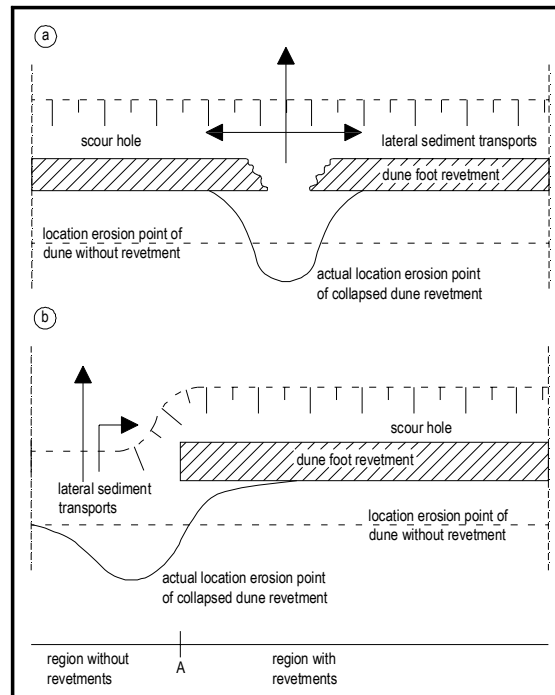


Figure 4.1 Schematic top-view of effects of hard elements on dune erosion at location where (a) revetment partially collapsed, and (b) seawall and sandy dune come together (according to Figure 4.54 in TAW, 1995)

However, in a 3D situation effects of dune revetments may still be present. For example at a location where the end of a seawall and a sandy dune come together (see Figure 4.1b) or at a location where a revetment has only partially collapsed (see Figure 4.1a), the erosion rate of the dune might be higher than in a situation where there are only dunes. The VTV provides some guidance on how to deal with these situations (see *e.g.* Figures 6-1.4 to 6-1.8 in Ministry of Transport, Public Works and Water Management, 2004). Since this guidance has not been verified with 3D physical model tests, it is recommended to perform a series of such tests.

4.3 Scour holes in safety assessment

The results of the measurements of the scour hole in Test T12 are analysed further into detail in this section. Results from previous investigations to scour holes are used for comparison. In WL | Delft Hydraulics (1988) several small- and large-scale tests are analysed to define characteristics of the depth and shape of scour holes in the vicinity of revetments. The development of scour holes appeared to be strongly related to the incident wave conditions, surge levels, beach slope and water depth near the toe. Other parameters that affect the size and depth of the scour hole are the sediment diameter, the water level variation during storm surge, the roughness of the revetment and the so-called top-erosion which is the supply of possibly available sediment from the top side of the revetment (TAW, 1995). Occurrence of top-erosion has a positive effect on the size of the scour hole; the depth will be smaller.

Results from tests with vertical revetments were not available for the analysis in WL | Delft Hydraulics (1988), only sloping revetments with different slope angles. It was concluded that for steeper revetments the initial development of the scour depth was faster than for

gentler revetments and that in case of steeper revetments some kind of equilibrium depth is reached sooner. This is clearly reflected in the results of the present tests, see Figure 3.4. The development of the scour depth is very fast in the first part of the test and much slower in the remainder of the test. It looks like an equilibrium depth is (almost) reached.

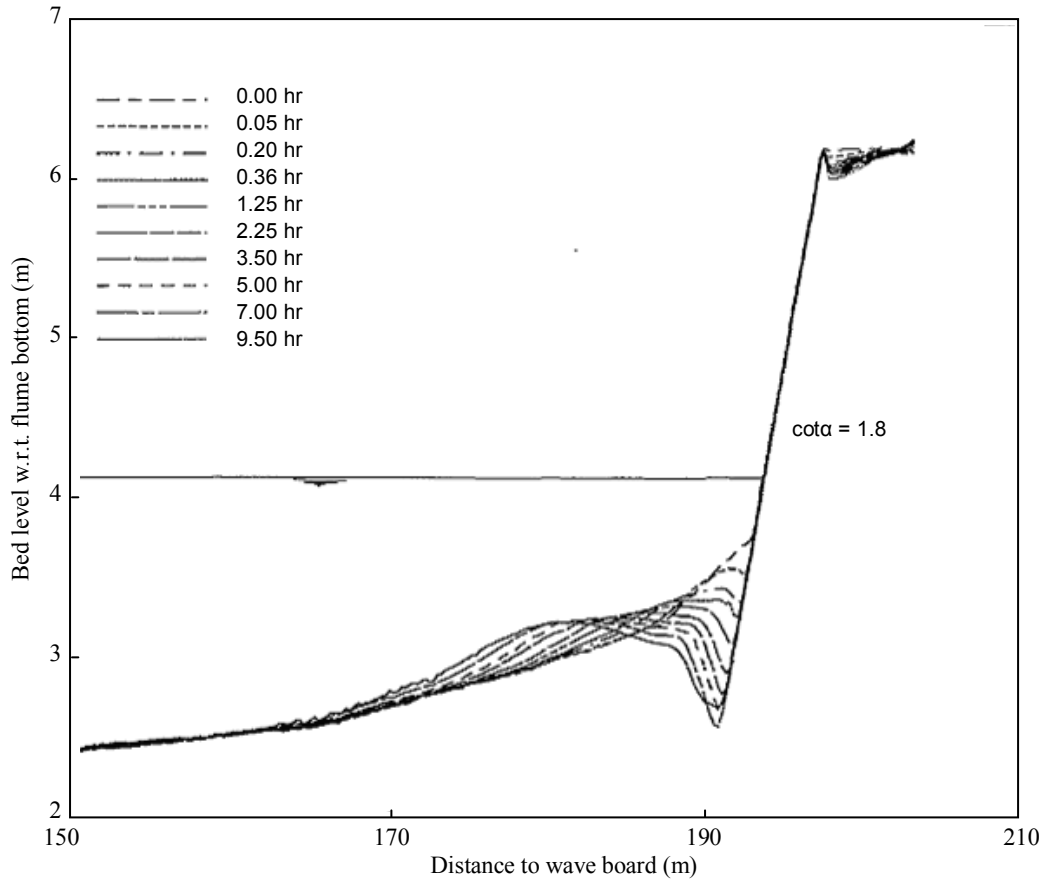


Figure 4.2 Profile development in Test T01 of research programme H0298 (WL | Delft Hydraulics, 1987a)

The maximum scour depth ($d_{s,max}$) and the wave height were expected to relate somehow for steeper revetments in WL | Delft Hydraulics (1988). Since the wave height is physically limited by the minimum water depth on the bar (h_b), the relative scour depth was considered to be an interesting parameter: $(d_{s,max} + h_i) / h_b$. Test T01 of research programme H0298 (WL | Delft Hydraulics, 1987a) was performed in the Delta flume at a depth scale of $n_d = 5$ with a revetment with a slope angle of $cota = 1.8$, see Figure 4.2. This test was performed on a scale close to Test T12 and had the steepest revetment compared to all other tests in WL | Delft Hydraulics (1988), which makes it most suitable for comparison with Test T12. The relative scour depth was found to increase until 7 hours to a value of about $(d_{s,max} + h_i) / h_b = 1.8$. In Test T12 the relative scour depth is constantly about $(d_{s,max} + h_i) / h_b = 1.5$; both the development and the value of the ratio are slightly different from the previous tests.

The location of the maximum scour depth was found to be closer to the revetment in the case of steeper revetments in WL | Delft Hydraulics (1988). The maximum scour depth was found directly next to the revetment in Test T12 in all measurements; this location did not

change in time (within the entire duration of the test). The maximum scour depth relative to the initial water depth in Test T12 seemed to reach an equilibrium value of $d_{s,max} / h_i \approx 2$; the scour depth is (almost) twice the initial water depth. In Test T01 of research programme H0298 the scour depth relative to the initial water depth after 7.0 hours is about $d_{s,max} / h_i \approx 1.7$ (h_i is determined at the location of $d_{s,max}$). However, the maximum scour depth (and the ratio with the initial water depth) did not seem to have reached an equilibrium value at that time, see Figure 4.2.

It should be noted that in the present test, wave overtopping very frequently occurred due to the (relatively) low freeboard. Dissipation of a part of the wave energy subsequently occurs on the horizontal part of the revetment and not at the vertical wall. It might therewith be reasoned that the scour hole could have developed differently if the freeboard was higher. A higher freeboard would have led to less wave overtopping and to more wave energy (or dissipation of energy) near the scour hole.

This information on the development and the dimensions of the scour hole at vertical revetments can be used in the assessment of the stability of the dune revetment. As mentioned in Section 4.2, the stability of the dune revetment is an important aspect in the assessment of the dune erosion at a location where dune revetments exist.

5 Conclusions and recommendations

5.1 Conclusions

Knowledge to take the influence of collapsed dune revetments (e.g. seaside boulevards, buildings, dune foot revetments, etc.) into account in the prediction of dune erosion is missing. In the current safety assessment method of the Dutch dunes, revetments in a cross-shore dune profile that fail during a storm are considered not to affect (positively or negatively) dune erosion under storm surge conditions compared to a dune profile without these elements. However, this assumption has never been verified with physical model tests. The objective of this study is to verify this assumption by performing large-scale physical model tests.

Large-scale tests were performed at a depth scale of $n_d = 6$ with the same hydraulic conditions as in Test T01 of earlier dune erosion tests (WL | Delft Hydraulics, 2006b). A wave height of $H_{m0} = 9$ m (prototype), wave period of $T_p = 12$ s (prototype) and sediment with a diameter of $D_{50} = 200$ μm were applied in the tests. Profile, wave and flow velocity measurements were carried out. In total four tests were carried out with two configurations of dune revetments:

- A dune with a geometry according to a reference profile covered with a revetment of loosely placed elements.
- A relatively low dune with a vertical revetment.

One test was performed with a collapsed revetment (Test T11) for the first configuration. A test from WL | Delft Hydraulics (2006b) was used for comparison with a situation without revetment. Three tests were performed with the second configuration: (1) a test without revetment (Test T14), (2) a test with a fixed revetment to study scour (Test T12), and (3) a test with a collapsed revetment (Test T13). These three tests were performed with the same (outer) geometry.

Based on the results of Tests T11 and T13 it can be concluded that for the tested geometries there are no important effects of a collapsed revetment on dune erosion in a 2D situation. It appeared that the erosion process for dunes with revetment is very similar to the erosion process of dunes without revetment, e.g. the rapid retreat of the dune face in the beginning of the storm and the logarithmic time-development of the erosion volume above the still water level can also be observed at dunes with revetment. Consequently, the dune erosion volume does not increase because of these elements and does not significantly decrease either. It seems legitimate to recommend the use of the standard safety assessment method for similar situations, therewith neglecting the presence of a revetment, under the condition that the remnant parts of the revetment are too small to cause 3D effects. If, however, the revetment only collapses over a limited section the erosion rate of the dune might be higher at this section where the revetment did collapse than in a situation where there are only dunes.

From Test T12 it becomes clear that a scour hole in front of a vertical revetment rapidly develops towards an equilibrium depth. The maximum scour depth relative to the initial water depth is $d_{s,max} / h_i \approx 2$ which is somewhat larger than the maximum scour depth found in other researches at sloping revetments.

5.2 Recommendations

The number of tests and therewith the range of validity, especially towards 3D situations, for the conclusions mentioned above are very limited, it is therefore recommended to perform additional physical model tests to extend the range of validity. Further analyses of the data and additional investigations to 3D aspects are necessary for the development of future guidelines. For example, the situations depicted in Figure 4.1 can be simulated in 3D small-scale physical model tests to investigate to what extent the cross-shore sediment transports are redirected laterally due to the scour holes in front of revetments and how this affects dune erosion.

In the present study dune revetments were assumed to fail during severe storm conditions. The strength of the dune revetment and the duration of the process of collapsing of the dune revetment itself, affect the total residual strength of the water defence. Especially for conditions for which the dune revetment would not fail or would only partially fail (*e.g.* during more frequently occurring storm conditions), it is relevant to verify whether the knowledge on the strength of dune revetments itself is sufficient.

From a comparison of the results of Tests T14 and T01 (WL | Delft Hydraulics, 2006b) it becomes clear that the shape of the initial profile somewhat affects the shape of the erosion profile (*e.g.* the slope of the erosion profile around and below the still water level). In the dune erosion prediction method by Vellinga (1986) the shape of the erosion profile solely depends on the hydraulic conditions and the fall velocity of the sediment. The influence of the initial profile on the erosion profile is not taken into account. It is recommended to further investigate the influence of the initial profile in relation with the storm duration on dune erosion with dedicated physical model tests.

References

- Borsboom, M.J.A., N. Doorn, J. Groeneweg and M.R.A. van Gent (2000), A Boussinesq-type model that conserves both mass and momentum. Proc. of 27th Int. Conf. on Coastal Engineering, pp. 148 – 161, Sydney, Australia.
- Borsboom, M.J.A., N. Doorn, J. Groeneweg and M.R.A. van Gent (2001), Near-shore wave simulations with a Boussinesq-type model including wave breaking. Proc. of 4th Coastal Dynamics Conference, pp. 759 – 768, Lund, Sweden.
- Dean, R.G. and R.A. Dalrymple (1991) Water Wave Mechanics for Engineers and Scientists, World Scientific. ISBN 981-02-0420-5
- Fowler, J.E. (1992), Scour problems and methods for prediction of maximum scour at vertical seawalls. T.R. CERC 92-16. U.S.W.E.S., Vicksburg, USA.
- Guza, R.T., E.B. Thornton, and R.A. Holman (1984), Swash on steep and shallow beaches. Proc. of 19th Int. Conf. on Coastal Engineering, pp. 708 - 723.
- Herbich, J.B. et al. (1965), Scour of flat sand beaches due to wave action in front of seawalls. Proc. Coastal Engineering, Santa Barbara Specialty Conference, ASCE.
- Holland, K.T. and R.A. Holman (1997), Video estimation of foreshore topography using trinocular stereo, Journal of Coastal Research, Vol. 13, No.1, pp.81-87.
- Holland, K.T., R.A. Holman, T.C. Lippmann, J. Stanley and N. Plant (1997), Practical use of video imagery in nearshore oceanographic field studies, IEEE Journal of Oceanic Engineering, Vol. 22, No.1, pp.81-92.
- Mansard, E.P.D. and E.R. Funke (1980), The measurement of incident and reflected spectra using a least-square method, Proc. of 17th Int. Conf. on Coastal Engineering, pp.154-172, ASCE, Sydney, Australia.
- Ministry of Transport, Public Works and Water Management (2004), The safety of the primary water defences in The Netherlands; Regulations for Safety Assessment for the second round of assessments 2001 – 2006 (VTV). (De veiligheid van de primaire waterkeringen in Nederland; Voorschrift Toetsen op Veiligheid voor de tweede toetsronde 2001 - 2006.) January 2004, DWW-2004-009, ISBN 90-369-5558-0 (in Dutch).
- Ribberink, J. S., and A. A. Al-Salem (1994), Sediment transport in oscillatory boundary layers in cases of rippled beds and sheet flow, J. Geophys. Res., 99(C6), 12,707–12,728.
- TAW (1995), Basic report Sandy Coast; Belonging to the Guidelines Sandy Coast. (Basisrapport Zandige Kust; Behorende bij de Leidraad Zandige Kust.) January 2005 (in Dutch).

- Van Gent, M.R.A. (2001), Wave run-up on dikes with shallow foreshores, ASCE, Journal of Waterway, Port, Coastal and Ocean Engineering, Vol. 127, No.5, Sept/Oct 2001, pp.254-262.
- Van Gent, M.R.A., and N. Doorn (2001), Numerical model simulations of wave propagation and wave run-up on dikes with shallow foreshores, Proc. of 4th Coastal Dynamics Conference, pp. 769 – 778, Lund, Sweden.
- Van Gent, M.R.A., A.J. Smale and C. Kuiper (2003), Stability of rock slopes with shallow foreshores, ASCE, Proc. of Coastal Structures, pp. 100-112, Portland.
- Van Rijn, L.C. (1998), Principles of coastal morphology. Aqua Publications, Amsterdam.
- WL | Delft Hydraulics (1982a), Dune erosion during super storm surge, northern beach Schouwen; investigation of the effectiveness of a dune revetment during super storm surge. (Duinafslag tijdens superstormvloed, Noorderstrand Schouwen; onderzoek naar de werking van een duinverdediging tijdens superstormvloed.) WL | Delft Hydraulics report M1797 (in Dutch).
- WL | Delft Hydraulics (1982b), Computational model for the estimation of dune erosion during storm surge. (Rekenmodel voor de verwachting van duinafslag tijdens stormvloed.) WL | Delft Hydraulics report M1263 part 4 (in Dutch).
- WL | Delft Hydraulics (1983), Investigations on the effectiveness of a dune revetment during super storm surge. (Oriënterend onderzoek naar de werking van een duinverdediging tijdens superstormvloed.) WL | Delft Hydraulics report M1819 part 3 (in Dutch).
- WL | Delft Hydraulics (1987a), Model research dune revetments; systematic investigation to the effectiveness of dune foot revetments; large-scale model research in Delta flume. (Modelonderzoek duinverdedigingen; systematisch onderzoek naar de werking van duinvoetverdedigingen; modelonderzoek op grote schaal in de Deltagoot.) WL | Delft Hydraulics report H0298 (in Dutch).
- WL | Delft Hydraulics (1987b), Systematic research to dune foot revetments; model research to erosion at the toe of dune foot revetment. (Systematisch onderzoek naar de werking van duinvoetverdedigingen; modelonderzoek naar de ontgroning van een duinvoetverdediging; modelonderzoek op grote schaal in de Deltagoot.) WL | Delft Hydraulics report M2051 part II (in Dutch).
- WL | Delft Hydraulics (1988), Scour holes; Analysis of relevant factors for the scour hole based on model tests and available literature. (Ontgrondingskuilen; Analyse van de voor de kuilvorm bepalende factoren op basis van uitgevoerd modelonderzoek en beschikbare literatuurgegevens.) WL | Delft Hydraulics report H0298 part 4 (in Dutch).
- WL | Delft Hydraulics (1995), LIP 11D Delta Flume Experiments; A dataset for profile validations. WL | Delft Hydraulics report H2130.

WL | Delft Hydraulics (1999), Physical model investigations on coastal structures with shallow foreshores; 2D model tests with single- and double-peaked wave energy spectra. WL | Delft Hydraulics report H3608.

WL | Delft Hydraulics (2006a), Dune erosion; Deterministic dune erosion prediction methods. WL | Delft Hydraulics report H4357, January 2006, Delft.

WL | Delft Hydraulics (2006b), Dune erosion; Large-scale model tests and dune erosion prediction method. WL | Delft Hydraulics report H4357, May 2006, Delft.

Tables

Test (-)	Speed (m/s)	Transect (m from wall)					
		1.25		2.5		3.75	
		start (m)	end (m)	start (m)	end (m)	start (m)	end (m)
T11A– T11E	0.15	27	225	27	225	27	225
T12A	0.15	27	225	27	225	27	225
T12B	0.15	-	-	27	225	-	-
	0.05	202	225	202	225	202	225
T12C	0.15	-	-	27	225	-	-
	0.05	192	225	192	225	192	225
T12D	0.15	-	-	27	225	-	-
	0.05	192	225	192	225	192	225
T12E	0.15	27	225	27	225	27	225
	0.05	202	225	202	225	202	225
T13A–T13E	0.15	27	225	27	225	27	225
T14A–T14E	0.15	27	225	27	225	27	225

Table A.1 Parts of profile that were measured in m from the wave board

Test	WHM01, WHM02, WHM03			
	H_{m0} (m)	T_p (s)	$T_{m-1,0}$ (s)	N (-)
T11A	1.37	4.7	4.6	88
T11B	1.44	5.0	4.7	178
T11C	1.39	4.9	4.6	656
T11D	1.40	5.0	4.6	964
T11E	1.40	4.9	4.6	3679
T12B	1.37	4.9	4.6	225
T12C	1.40	4.8	4.6	672
T12D	1.36	4.9	4.6	970
T12E	1.36	4.9	4.6	3674
T13A	1.37	4.8	4.6	85
T13B	1.41	5.0	4.7	182
T13C	1.37	4.9	4.6	654
T13D	1.37	4.9	4.6	968
T13E	1.38	4.9	4.6	3689
T14A	1.39	4.7	4.7	86
T14B	1.44	5.0	4.7	182
T14C	1.35	4.9	4.6	652
T14D	1.37	5.0	4.6	973
T14E	1.36	4.9	4.6	3684

Table A.2 Incident wave conditions measured with wave height meters WHM01, WHM02 and WHM03

Test	WHM01			WHM02			WHM03		
	H_{m0} (m)	T_p (s)	$T_{m-1,0}$ (s)	H_{m0} (m)	T_p (s)	$T_{m-1,0}$ (s)	H_{m0} (m)	T_p (s)	$T_{m-1,0}$ (s)
T11A	1.40	4.5	4.9	1.39	4.6	5.0	1.40	4.7	5.0
T11B	1.49	4.9	5.1	1.48	4.9	5.1	1.48	5.1	5.2
T11C	1.44	4.8	5.0	1.43	4.9	5.1	1.42	5.0	5.2
T11D	1.42	4.9	5.0	1.41	5.0	5.0	1.41	5.0	5.1
T11E	1.42	4.9	5.0	1.41	4.9	5.0	1.42	4.9	5.0
T12B	1.42	4.8	5.1	1.41	4.9	5.2	1.42	5.0	5.3
T12C	1.46	4.8	5.1	1.44	4.9	5.2	1.44	4.9	5.3
T12D	1.42	5.0	4.9	1.42	5.0	5.0	1.41	5.0	5.0
T12E	1.42	4.9	4.9	1.42	5.0	4.9	1.41	5.0	5.0
T13A	1.45	4.7	5.0	1.41	4.6	5.1	1.43	4.8	5.1
T13B	1.48	5.0	5.0	1.47	5.1	5.1	1.47	5.0	5.3
T13C	1.39	4.8	4.9	1.39	4.9	4.9	1.39	4.9	5.0
T13D	1.40	5.0	4.9	1.40	5.0	4.9	1.41	5.0	4.9
T13E	1.41	4.9	4.8	1.40	4.9	4.9	1.41	4.9	4.9
T14A	1.45	4.7	5.4	1.45	4.7	5.2	1.42	4.9	5.6
T14B	1.47	5.0	5.1	1.47	5.0	5.0	1.43	5.0	5.2
T14C	1.38	4.8	4.9	1.38	4.9	4.9	1.36	4.9	5.0
T14D	1.39	5.0	5.0	1.40	5.0	4.9	1.38	5.0	5.0
T14E	1.38	4.9	4.9	1.40	4.9	5.0	1.37	5.0	5.0

Table A.3 Wave conditions measured with wave height meters WHM01, WHM02 and WHM03

Test	PS01 & EMS01		
	H_{m0} (m)	T_p (s)	$T_{m-1,0}$ (s)
T11A	1.42	4.9	4.7
T11B	1.49	4.9	4.7
T11C	1.44	5.0	4.5
T11D	1.45	4.9	4.5
T11E	1.45	4.9	4.5
T12B	1.47	5.0	4.9
T12C	1.52	5.0	4.9
T12D	1.43	4.9	4.5
T12E	1.43	4.8	4.5
T13A	1.43	4.8	4.9
T13B	1.45	4.8	5.1
T13C	1.42	5.0	4.6
T13D	1.43	4.8	4.4
T13E	1.43	5.0	4.5
T14A	1.45	4.8	4.9
T14B	1.47	4.8	5.0
T14C	1.42	5.0	4.6
T14D	1.43	4.8	4.4
T14E	1.44	5.0	4.5

Table A.4 Incident wave conditions measured with pressure sensor PS01 and flow velocity meter EMS01

Test	PS01			PS02			PS03		
	H_{m0} (m)	T_p (s)	$T_{m-1,0}$ (s)	H_{m0} (m)	T_p (s)	$T_{m-1,0}$ (s)	H_{m0} (m)	T_p (s)	$T_{m-1,0}$ (s)
T11A	1.52	4.9	4.6	1.44	4.9	4.7	1.24	4.9	5.6
T11B	1.61	4.9	4.6	1.52	4.9	4.6	1.28	4.9	5.2
T11C	1.56	4.9	4.5	1.47	4.9	4.5	1.24	4.9	5.1
T11D	1.53	5.0	4.3	1.45	5.0	4.2	1.21	5.5	4.6
T11E	1.53	4.8	4.4	1.42	4.7	4.4	1.20	5.1	4.8
T12B	1.59	4.9	4.6	1.50	4.9	4.4	1.26	4.9	5.0
T12C	1.63	4.9	4.7	1.49	4.9	4.6	1.26	5.6	5.1
T12D	1.59	5.0	4.2	1.48	5.0	4.2	1.25	5.0	4.6
T12E	1.59	4.7	4.4	1.49	4.9	4.4	1.25	5.1	4.9
T13A	1.52	4.7	5.0	1.42	4.7	4.8	1.23	4.7	5.3
T13B	1.55	4.7	4.9	1.43	4.7	5.0	1.22	4.7	5.4
T13C	1.50	4.9	4.5	1.39	4.9	4.5	1.19	4.9	5.0
T13D	1.52	4.9	4.3	1.42	4.9	4.2	1.20	5.1	4.7
T13E	1.50	4.8	4.4	1.41	4.7	4.3	1.19	5.1	4.8
T14A	1.53	4.7	4.7	1.45	4.7	4.8	1.26	4.7	5.1
T14B	1.57	4.7	4.8	1.46	4.7	4.7	1.23	4.7	5.2
T14C	1.50	4.9	4.5	1.43	4.9	4.5	1.19	4.9	5.0
T14D	1.53	5.1	4.4	1.45	4.9	4.3	1.20	5.1	4.8
T14E	1.53	4.7	4.4	1.45	4.7	4.4	1.20	4.7	4.9

Table A.5 Wave conditions measured with pressure sensors PS01 – PS03

Test	PS04			PS05			PS06		
	H_{m0} (m)	T_p (s)	$T_{m-1,0}$ (s)	H_{m0} (m)	T_p (s)	$T_{m-1,0}$ (s)	H_{m0} (m)	T_p (s)	$T_{m-1,0}$ (s)
T11A	1.13	4.9	5.6	1.08	4.1	5.9	0.96	4.1	5.6
T11B	1.19	4.9	5.5	1.15	4.9	5.6	1.02	6.0	5.8
T11C	1.15	4.9	5.6	1.11	5.7	5.6	1.00	5.7	5.4
T11D	1.12	5.5	4.9	1.08	6.1	4.8	0.96	6.1	4.9
T11E	1.11	5.8	5.0	1.07	6.0	5.3	0.95	6.0	5.4
T12B	1.15	4.9	5.3	1.12	6.1	5.4	0.99	3.6	5.4
T12C	1.16	5.6	5.8	1.11	5.6	5.7	0.99	5.6	6.2
T12D	1.16	5.5	4.8	1.12	6.1	4.6	1.00	5.5	5.0
T12E	1.17	5.7	5.2	1.13	6.1	5.3	1.02	5.4	5.2
T13A	1.15	4.7	5.6	1.09	4.7	5.9	0.98	4.2	6.0
T13B	1.14	4.7	6.0	1.08	4.7	6.0	0.99	6.2	6.8
T13C	1.11	4.9	5.3	1.05	4.9	5.5	0.96	4.9	5.3
T13D	1.12	6.0	4.8	1.07	6.0	5.0	0.95	6.0	5.0
T13E	1.11	5.8	4.9	1.07	5.8	5.0	0.95	6.0	5.2
T14A	1.15	4.7	5.2	1.07	4.7	5.7	0.99	4.7	5.9
T14B	1.13	4.7	5.4	1.06	4.7	5.6	0.97	4.7	6.2
T14C	1.11	4.9	5.3	1.03	4.9	5.6	0.95	4.9	5.5
T14D	1.12	6.0	5.0	1.05	6.0	5.0	0.96	6.0	5.2
T14E	1.12	5.8	5.1	1.06	5.8	5.2	0.96	6.0	5.6

Table A.6 Wave conditions measured with pressure sensors PS04 – PS06

Test	PS07			PS08			PS09		
	H_{m0} (m)	T_p (s)	$T_{m-1,0}$ (s)	H_{m0} (m)	T_p (s)	$T_{m-1,0}$ (s)	H_{m0} (m)	T_p (s)	$T_{m-1,0}$ (s)
T11A	0.74	5.5	6.5	0.77	5.9	8.2	0.74	30.9	11.8
T11B	0.89	6.0	6.1	0.80	6.0	8.6	0.77	22.7	11.8
T11C	0.84	6.2	6.5	0.76	6.2	9.6	0.68	28.2	13.7
T11D	0.78	5.0	5.5	0.62	34.7	6.6	0.52	34.7	11.4
T11E	0.78	5.5	6.0	0.52	36.5	9.7	0.46	36.5	17.2
T12B	0.81	6.1	5.9	0.74	33.8	8.7	0.77	20.4	11.7
T12C	0.82	5.6	7.7	0.73	24.3	10.5	0.75	24.3	12.7
T12D	0.83	5.5	4.9	0.75	34.7	6.1	0.75	20.9	8.9
T12E	0.83	5.4	5.8	0.73	28.7	8.7	0.75	18.2	10.8
T13A	0.80	6.2	7.8	0.70	6.2	11.9	0.68	11.4	17.3
T13B	0.78	6.2	8.0	0.69	26.4	11.4	0.56	26.4	16.7
T13C	0.75	4.9	6.2	0.63	46.8	9.2	0.47	28.2	14.6
T13D	0.75	4.9	5.6	0.56	7.2	7.0	0.44	41.6	9.6
T13E	0.78	5.5	5.9	0.53	16.1	7.6	0.43	36.5	10.5
T14A	0.79	6.2	7.6	0.67	6.2	11.5	0.66	11.4	14.7
T14B	0.77	6.2	7.8	0.70	6.2	10.2	0.53	26.5	16.4
T14C	0.77	4.9	6.0	0.63	15.7	9.1	0.48	46.8	14.4
T14D	0.75	5.4	6.2	0.59	16.1	7.6	0.48	41.6	9.6
T14E	0.80	5.5	6.4	0.56	16.1	8.3	0.47	36.5	10.9

Table A.7 Wave conditions measured with pressure sensors PS07 – PS09

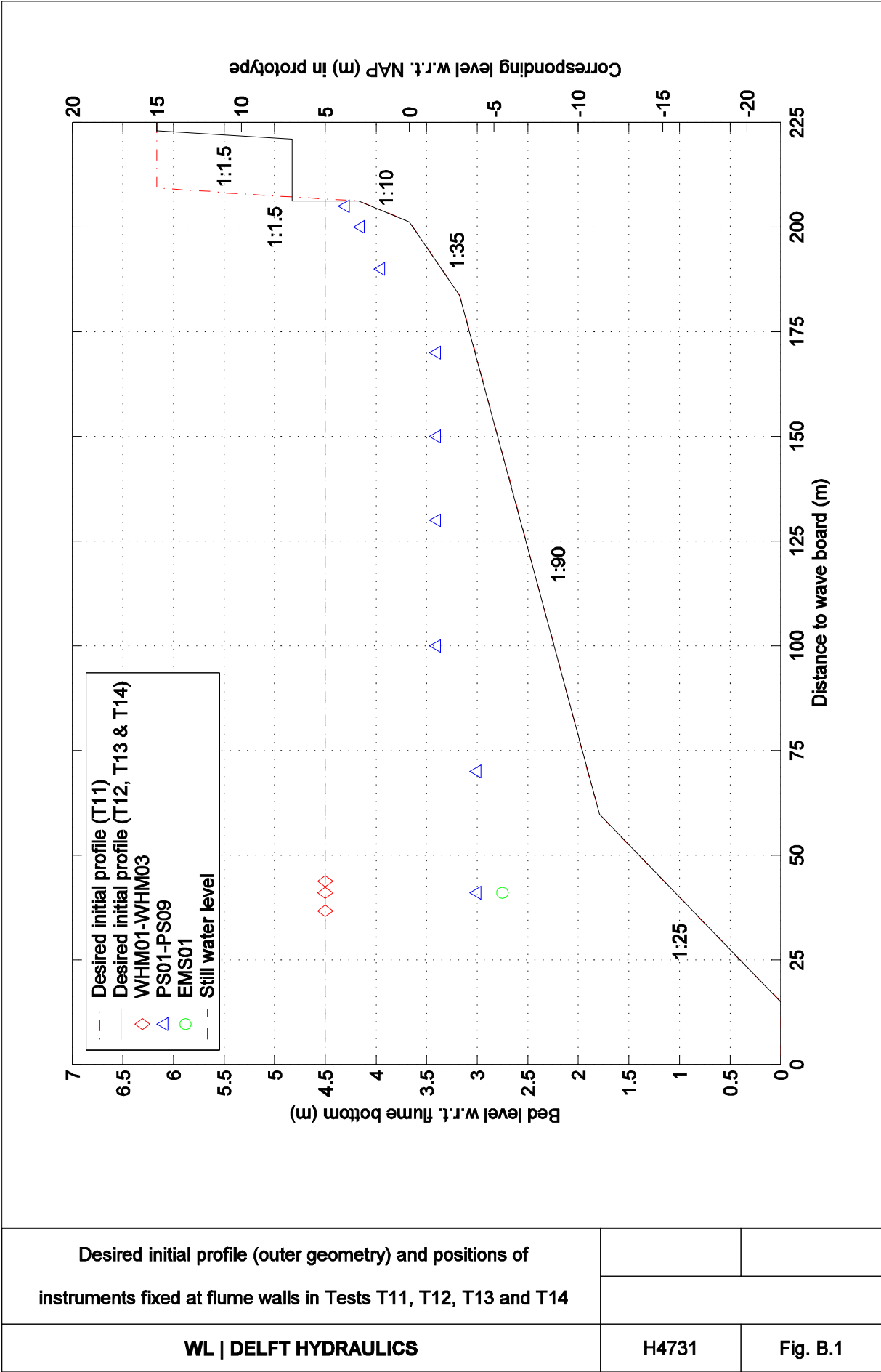
Test	Temperature (°C)
T11A	11.2
T11B	10.9
T11C	10.7
T11D	10.7
T11E	10.8
Average T11	10.9
T12B	13.9
T12C	14.3
T12D	13.7
T12E	13.7
Average T12	13.9
T13A	13.7
T13B	13.3
T13C	13.3
T13D	13.1
T13E	13.1
Average T13	13.3
T14A	14.3
T14B	15.4
T14C	15.4
T14D	15.4
T14E	15.4
Average T14	15.2

Table A.8 Measured water temperatures

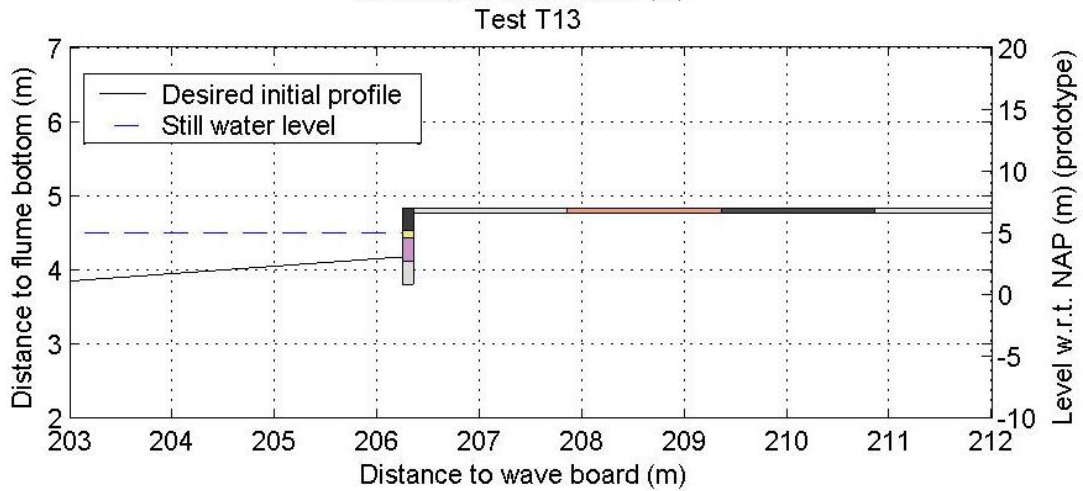
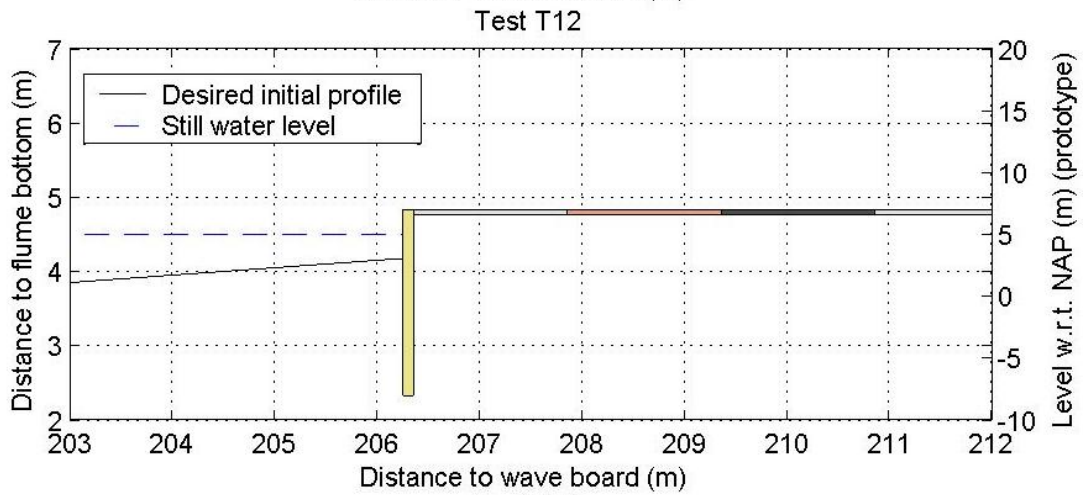
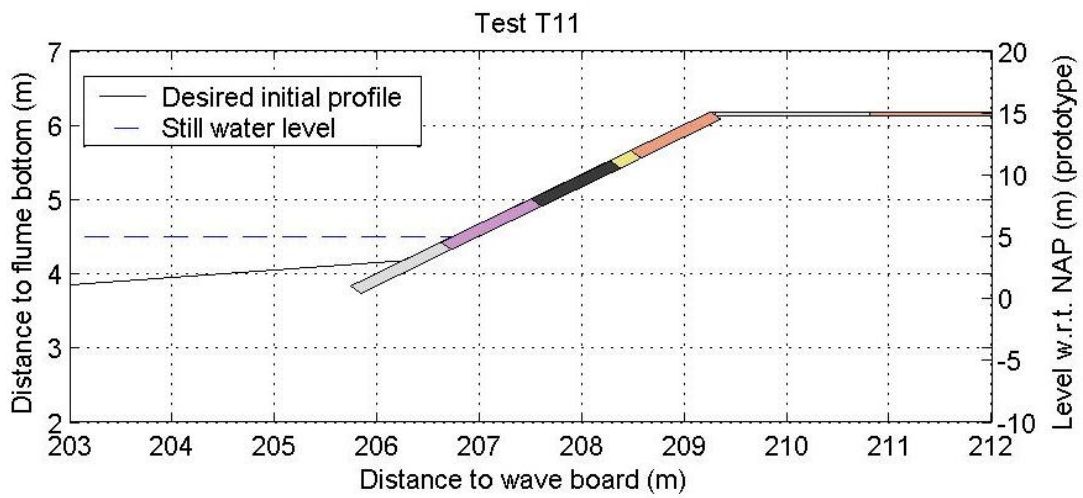
Element (-)	Sample (-)	Mass (kg)	Density (kg/m³)
Blocks (0.1 m · 0.1 m · 0.08 m)	1	1.88	2309
	2	1.98	2387
	3	1.93	2369
	4	1.86	2295
	5	1.91	2372
	6	1.86	2311
	7	1.91	2385
	8	1.90	2373
	9	1.97	2387
	10	1.98	2352
	11	1.99	2357
	12	1.96	2348
	Average	1.93	2354
Bricks (0.2 m · 0.1 m · 0.08 m)	1	4.00	2353
	2	4.00	2353
	3	4.05	2382
	4	4.10	2412
	Average	4.04	2375
Tiles (0.3 m · 0.3 m · 0.05 m)	1	8.95	2183
	2	8.95	2183
	3	8.80	2228
	4	9.00	2222
	5	8.65	2218
	6	9.10	2220
	Average	8.91	2209

Table A.9 Masses and densities of structure elements

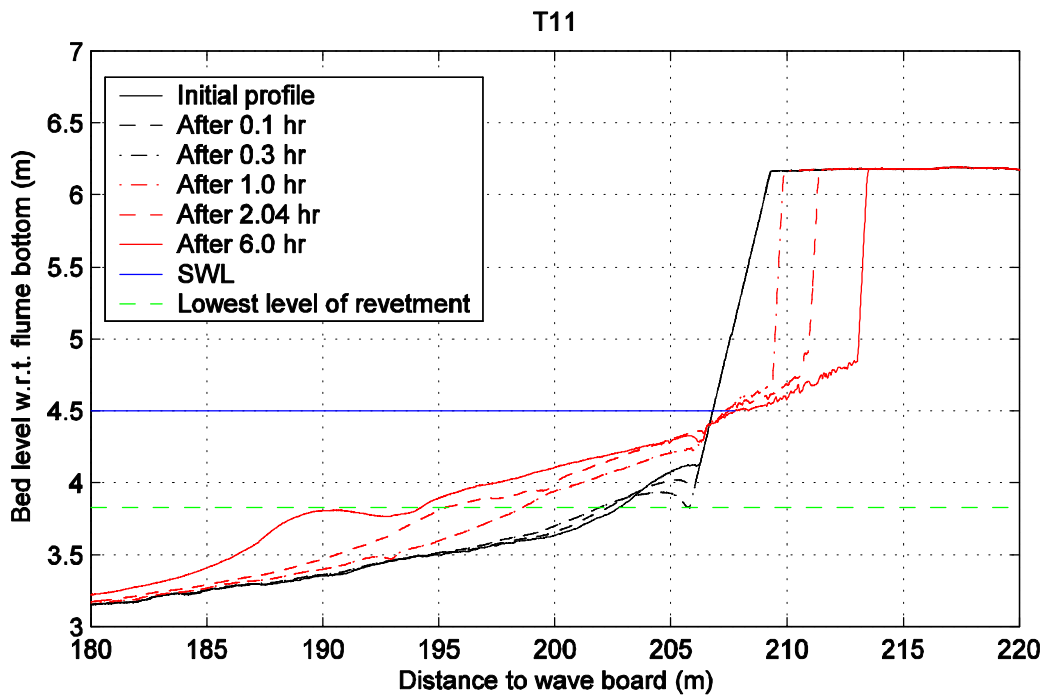
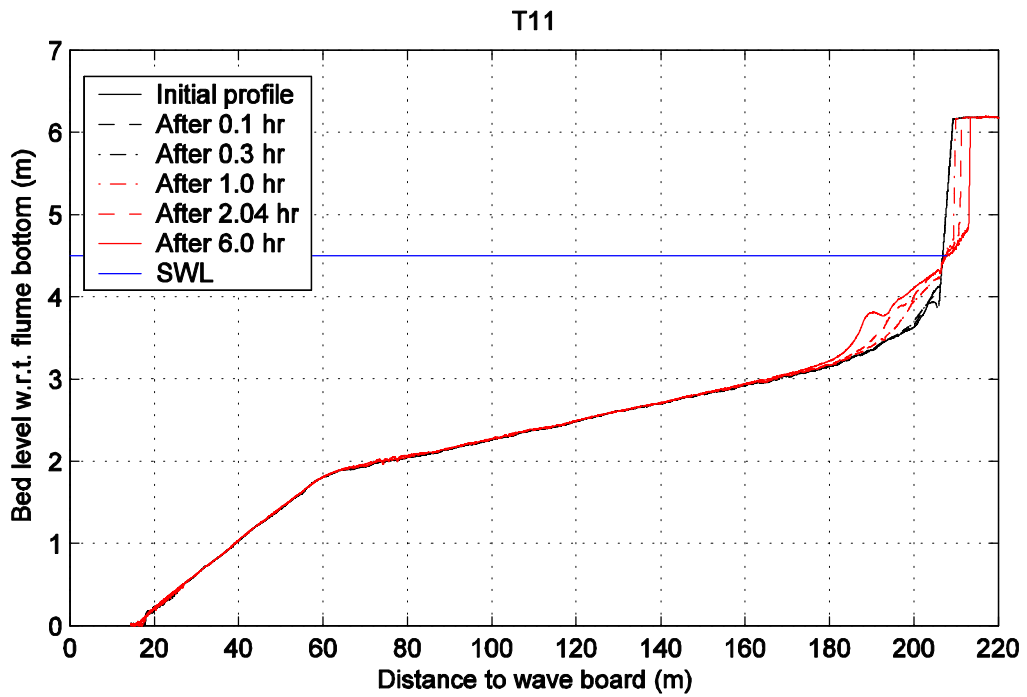
Figures



<p>Desired initial profile (outer geometry) and positions of instruments fixed at flume walls in Tests T11, T12, T13 and T14</p>		
	<p>WL DELFT HYDRAULICS</p>	<p>H4731</p>



Revetments in Tests T11, T12 and T13



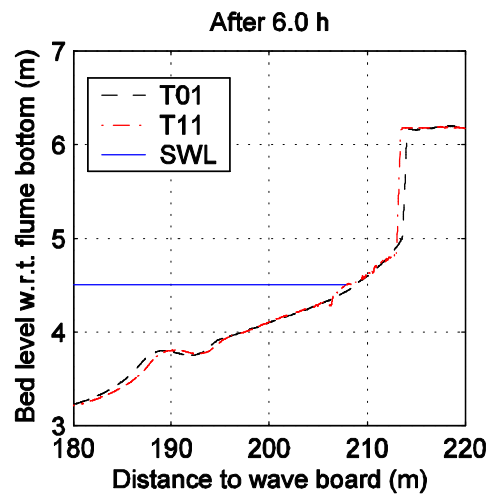
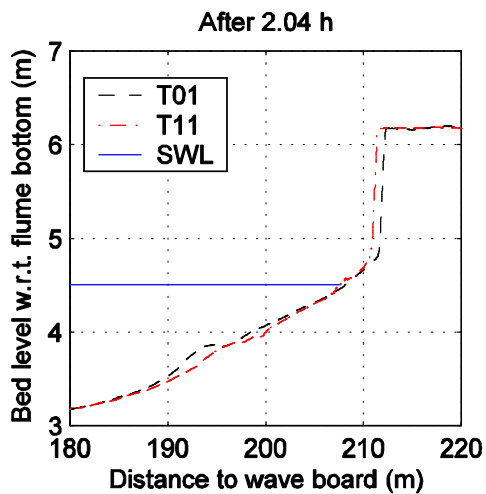
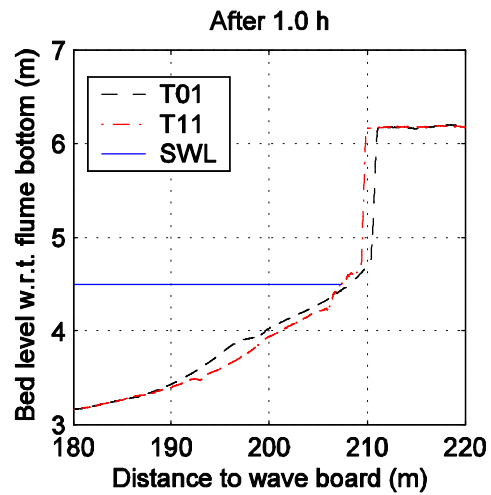
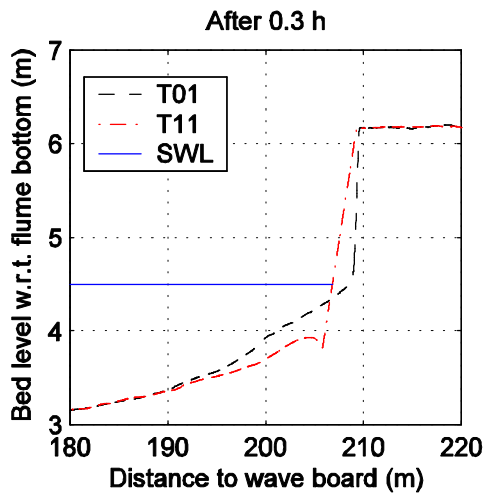
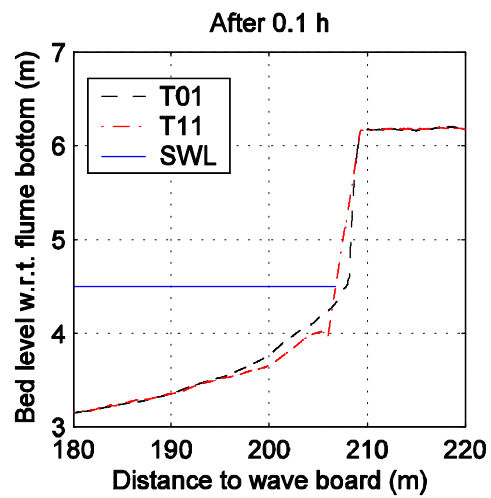
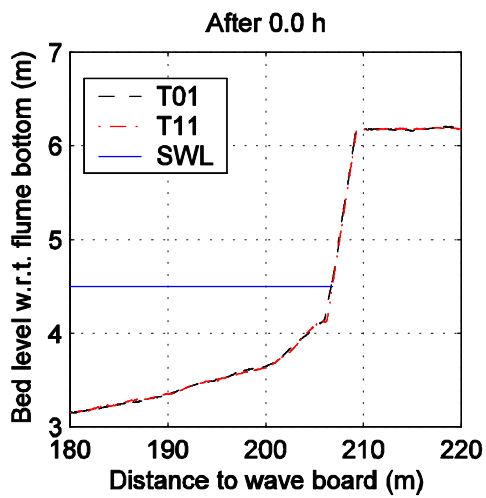
Development of average cross-shore profiles

Test T11

WL | DELFT HYDRAULICS

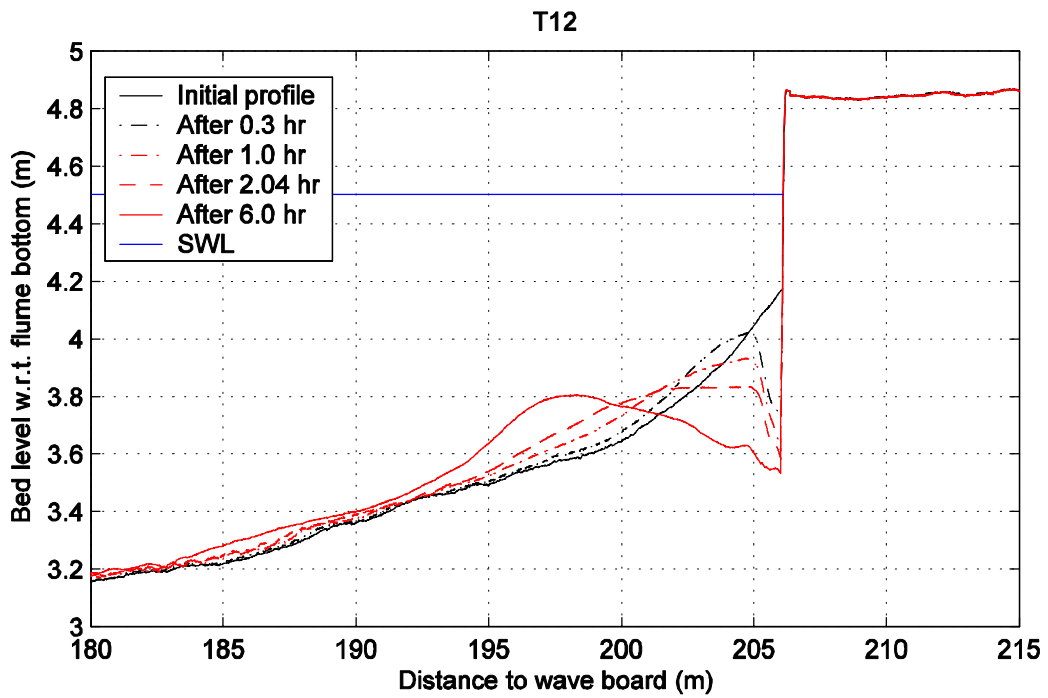
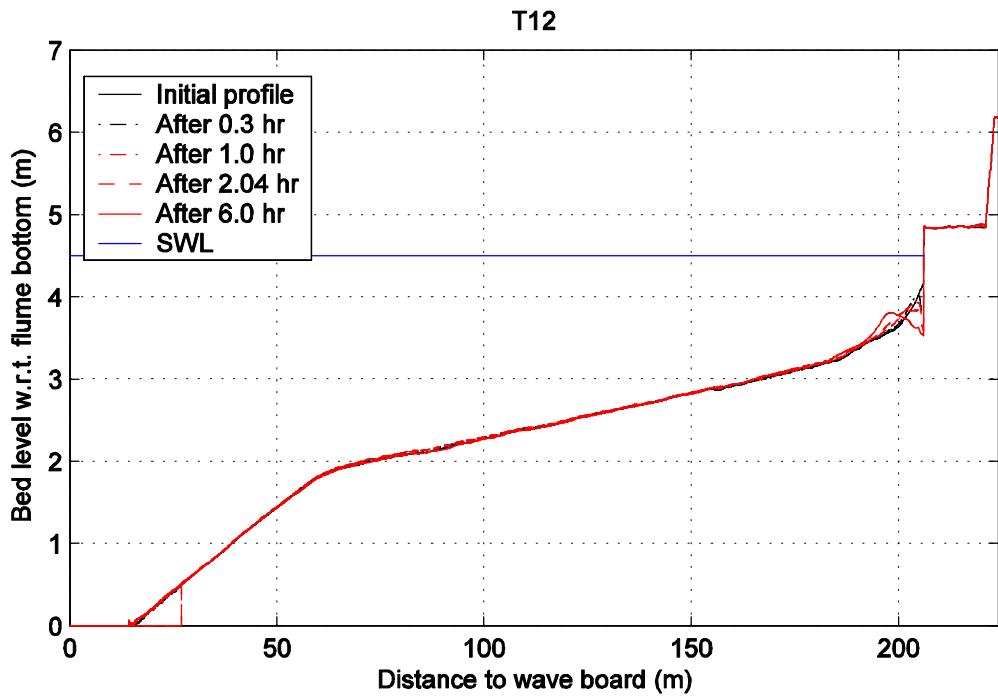
H4731

Fig. B.3



Comparison of average cross-shore profiles of tests with equal hydraulic conditions and initial profiles (outer geometry)

Tests T01 & T11



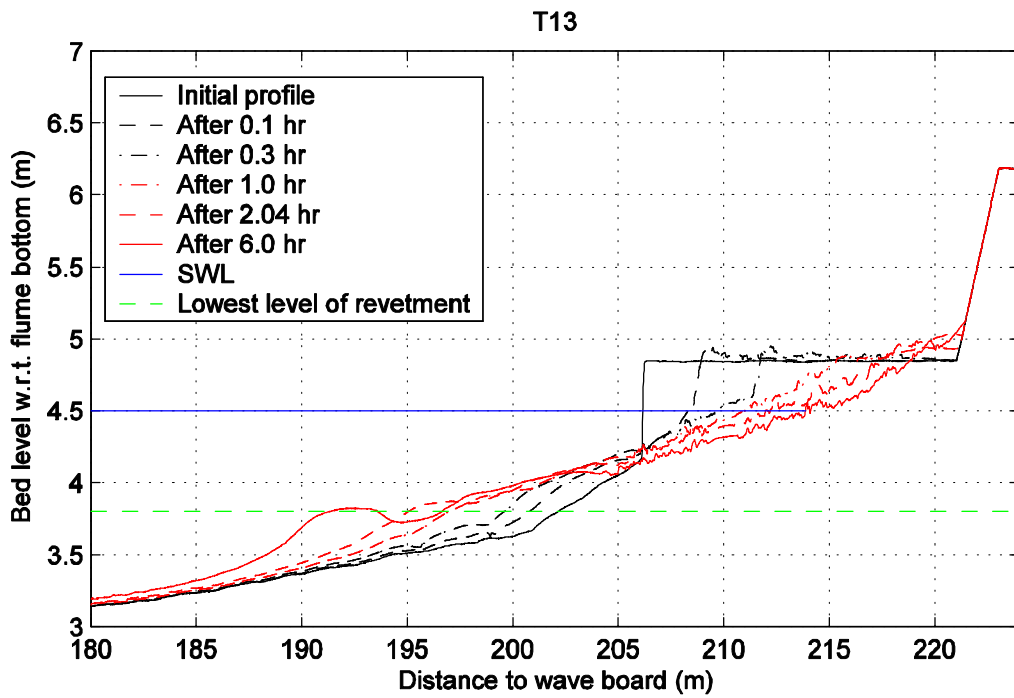
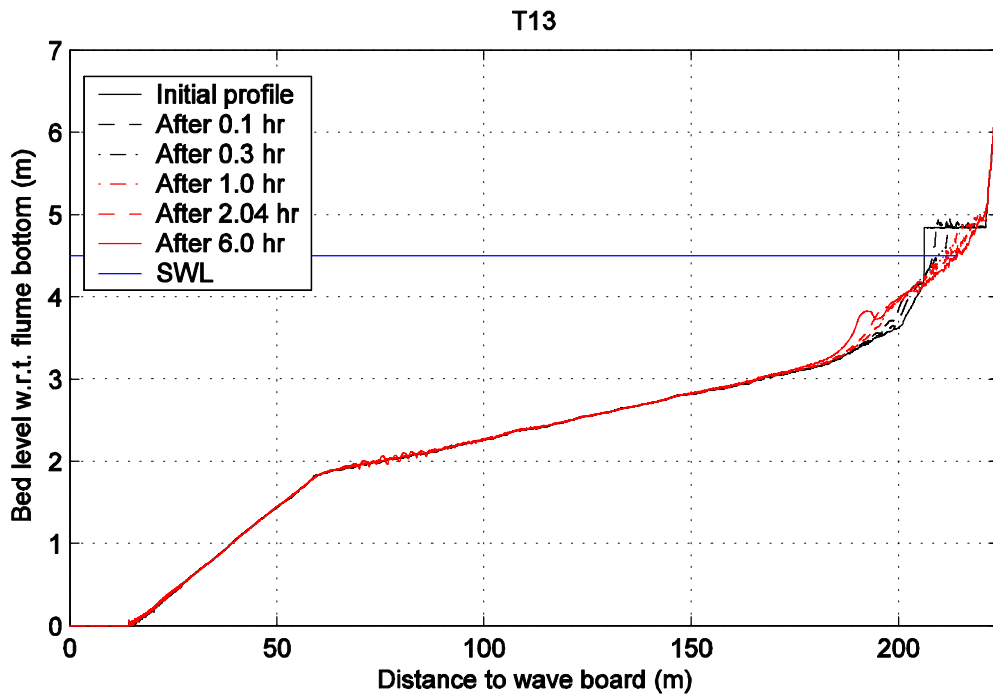
Development of average cross-shore profiles

Test T12

WL | DELFT HYDRAULICS

H4731

Fig. B.5



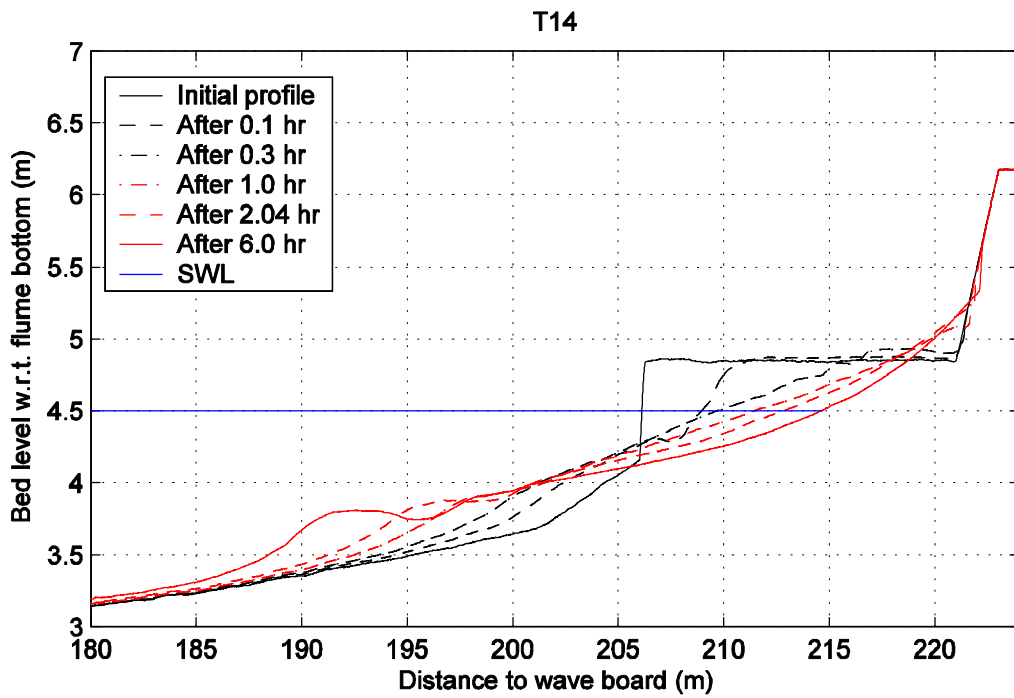
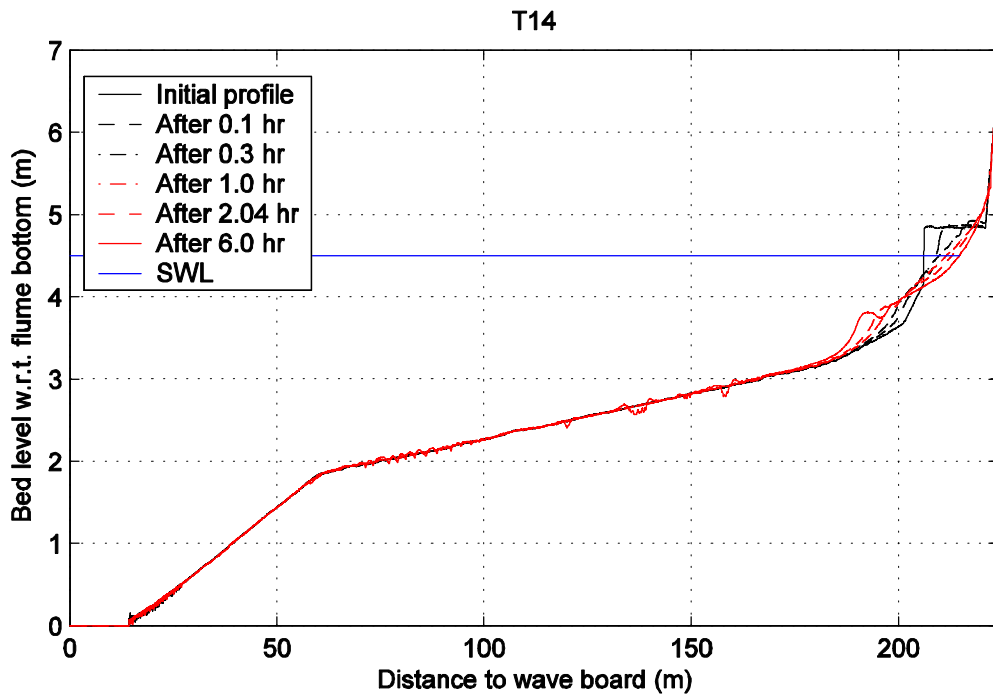
Development of average cross-shore profiles

Test T13

WL | DELFT HYDRAULICS

H4731

Fig. B.6



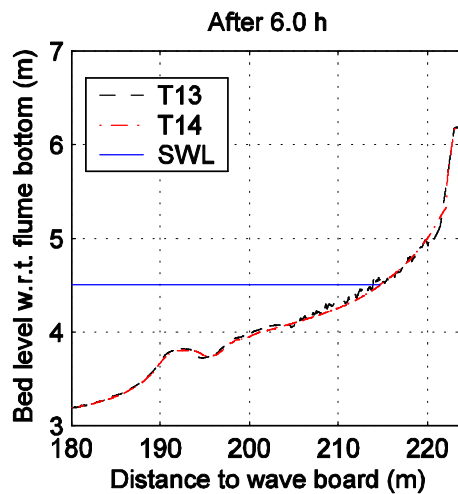
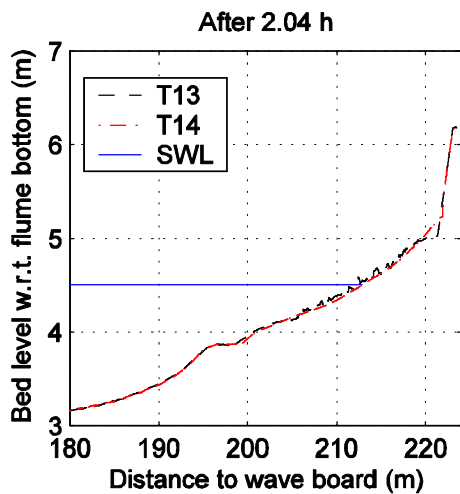
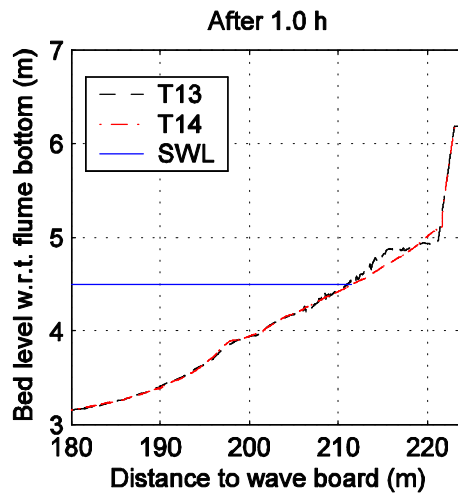
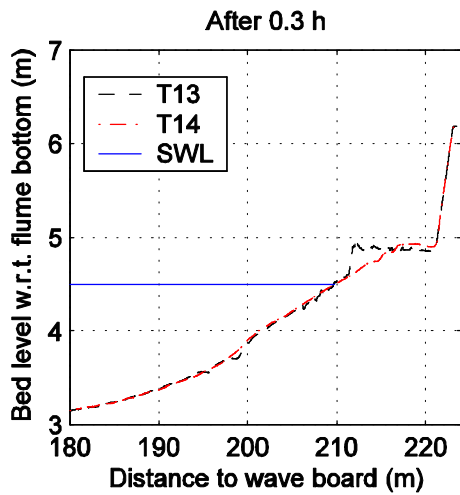
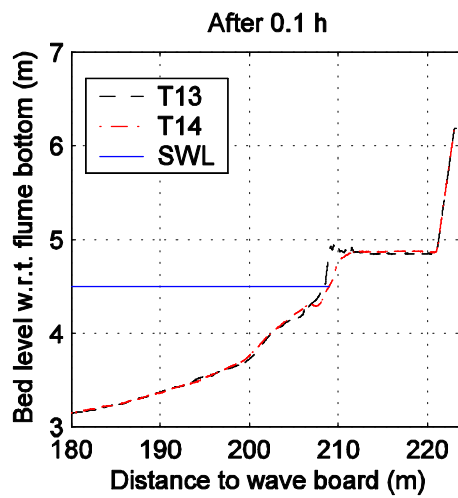
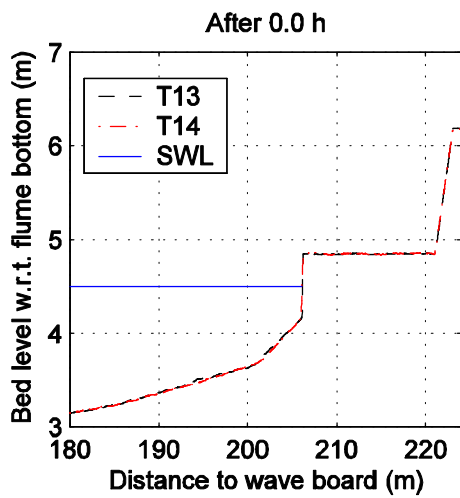
Development of average cross-shore profiles

Test T14

WL | DELFT HYDRAULICS

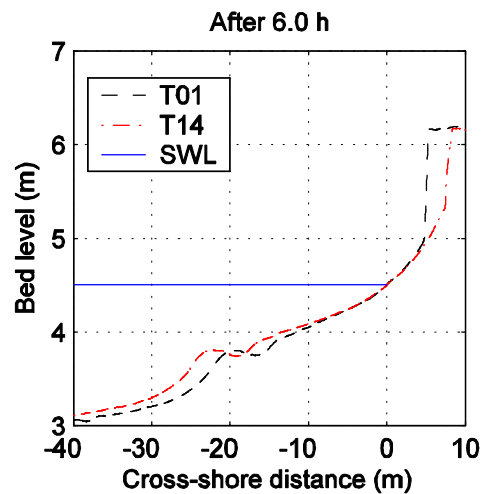
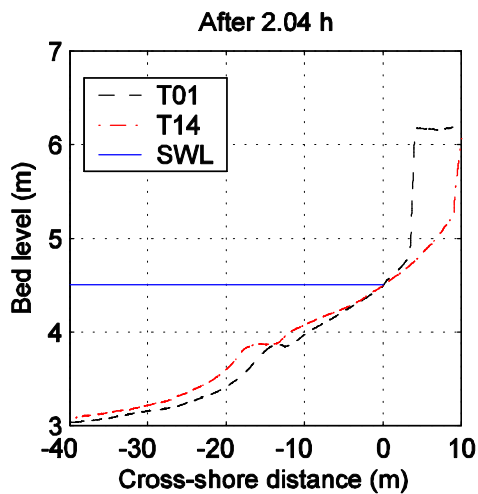
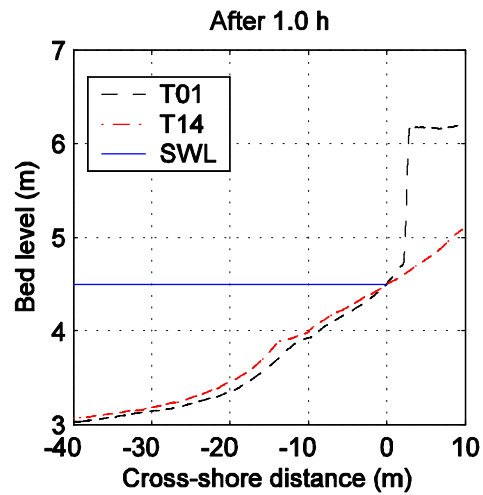
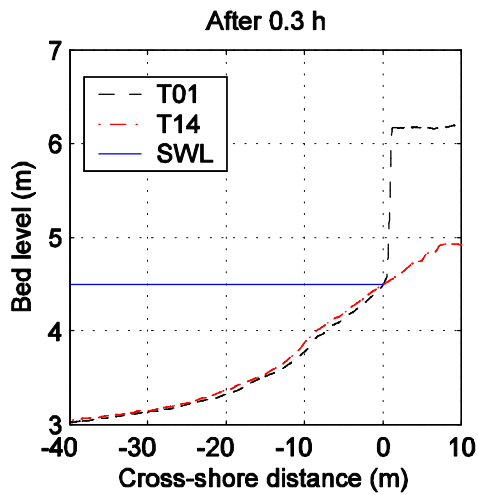
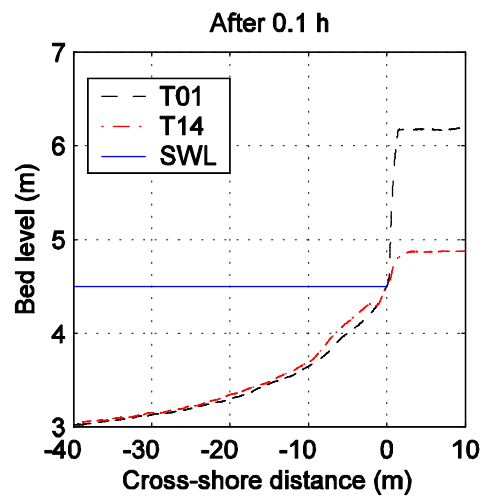
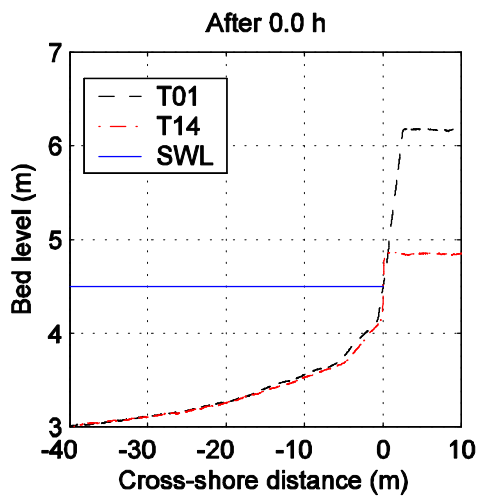
H4731

Fig. B.7



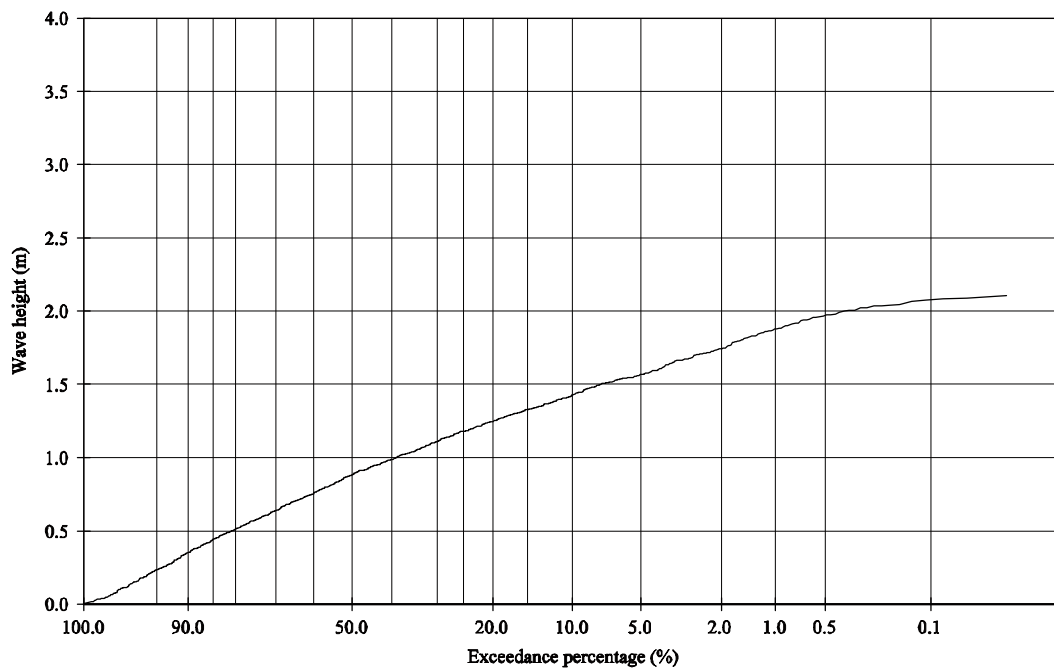
Comparison of average cross-shore profiles of tests with equal hydraulic conditions and initial profiles (outer geometry)

Tests T13 & T14

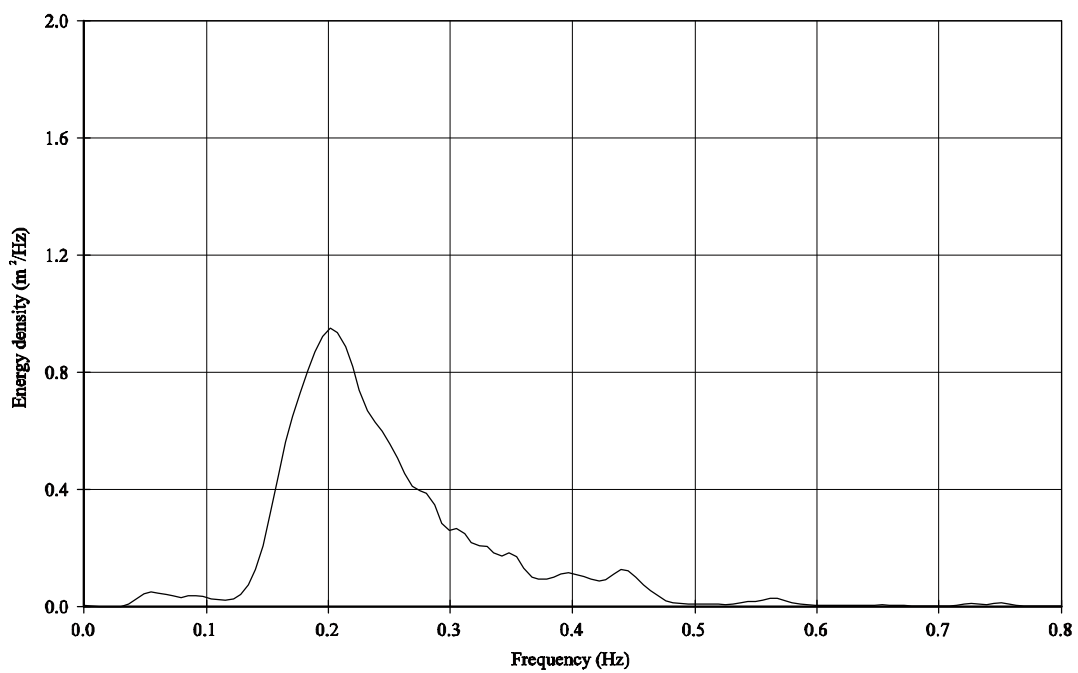


Comparison of average (horizontally translated) cross-shore profiles
of tests with equal hydraulic conditions

Tests T01 & T14



— Incident



Wave height exceedance curve and
energy density spectrum

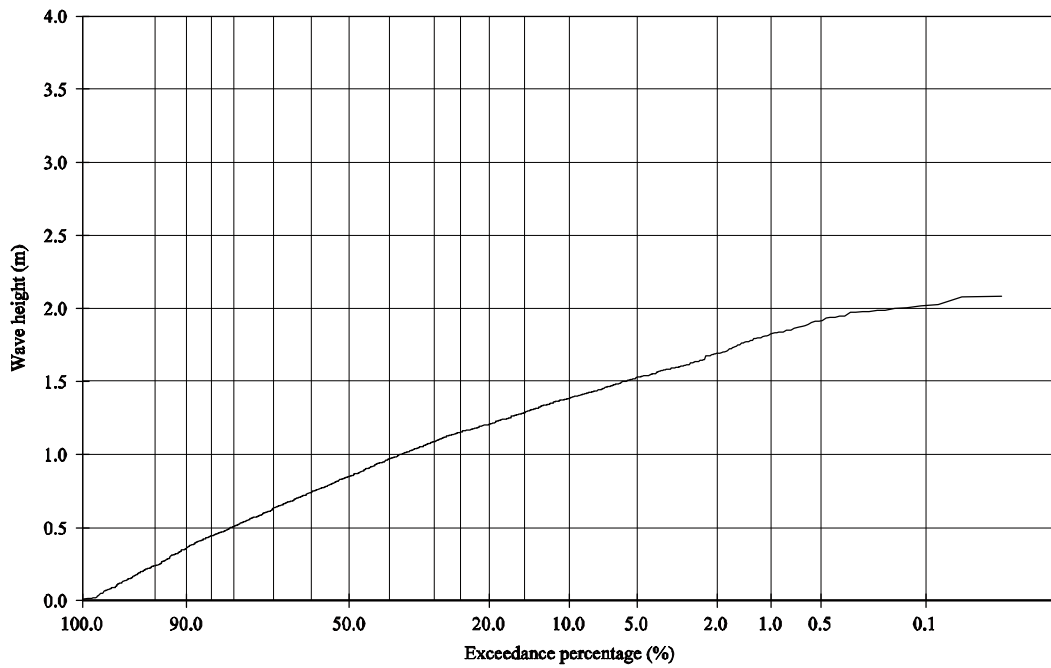
T11E

Incident

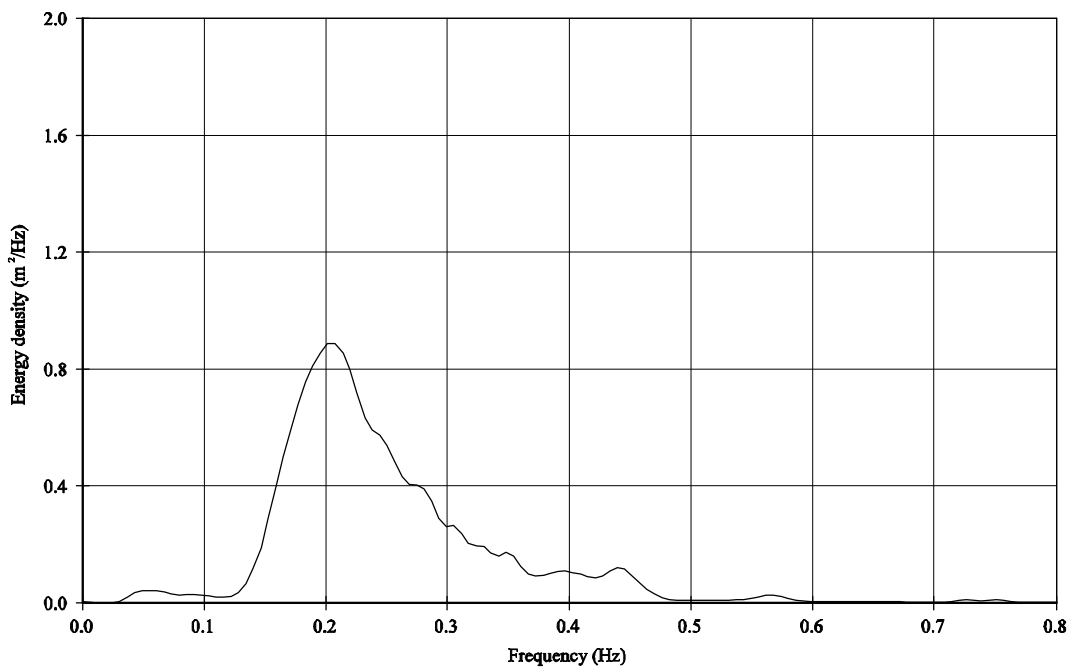
WL/Delft Hydraulics

H4731

Fig. B.10



— Incident



Wave height exceedance curve and
energy density spectrum

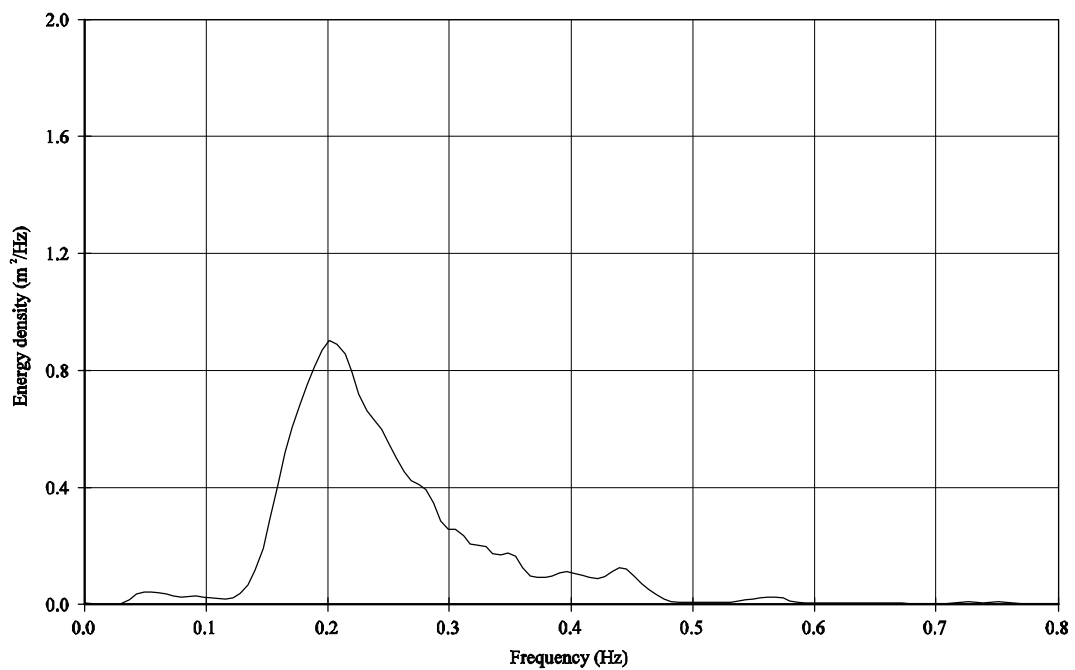
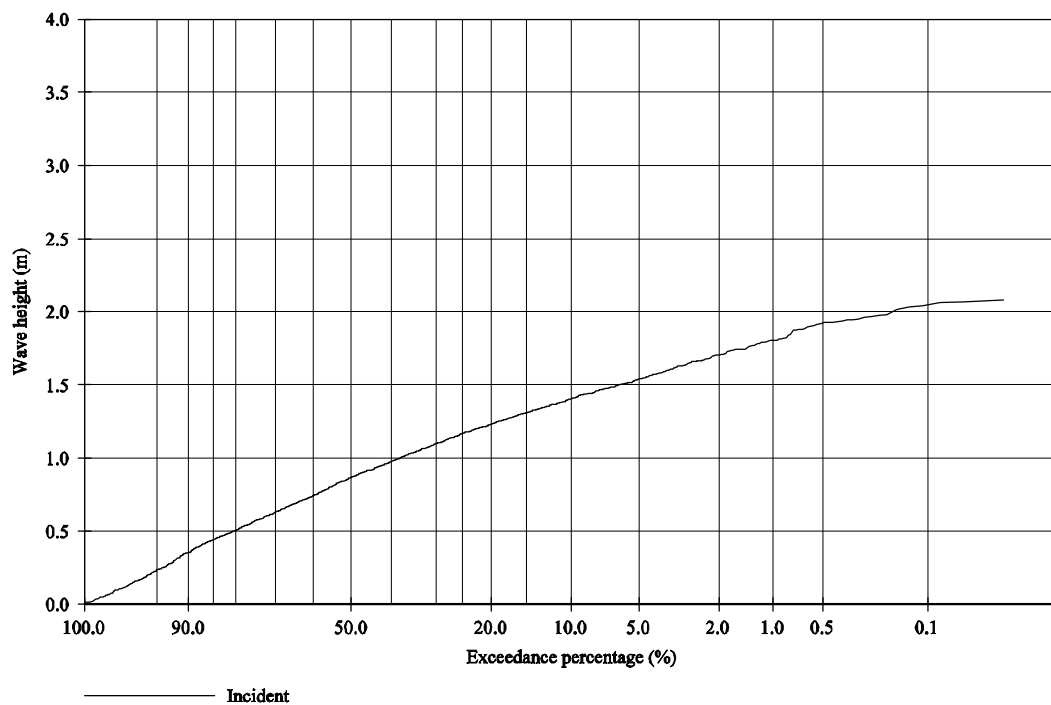
T12E

Incident

WL/Delft Hydraulics

H4731

Fig. B.11



Wave height exceedance curve and
energy density spectrum

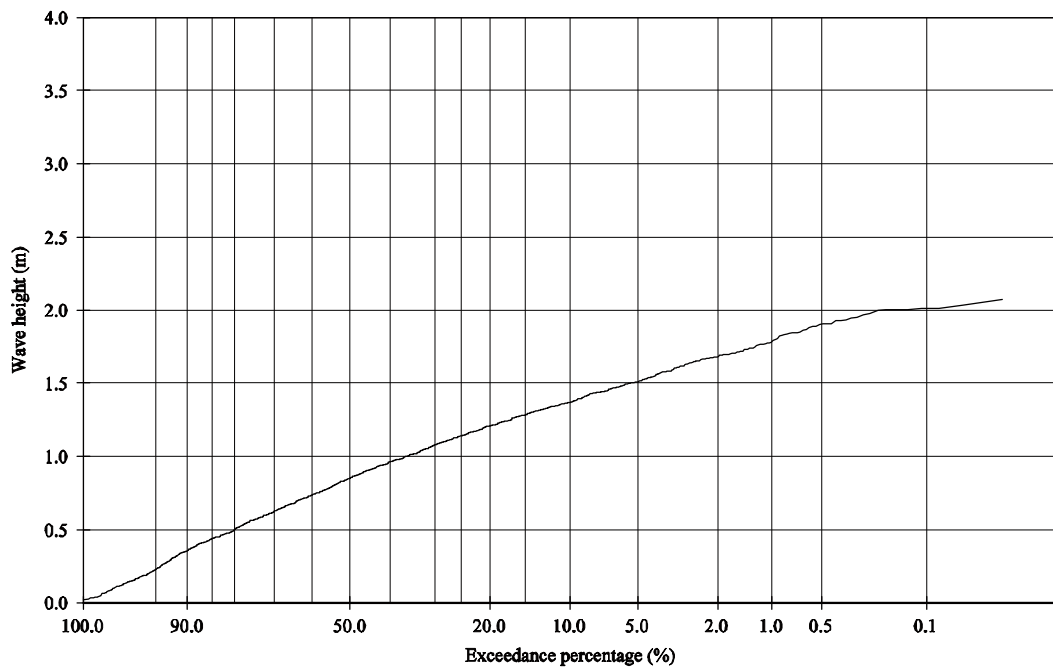
T13E

Incident

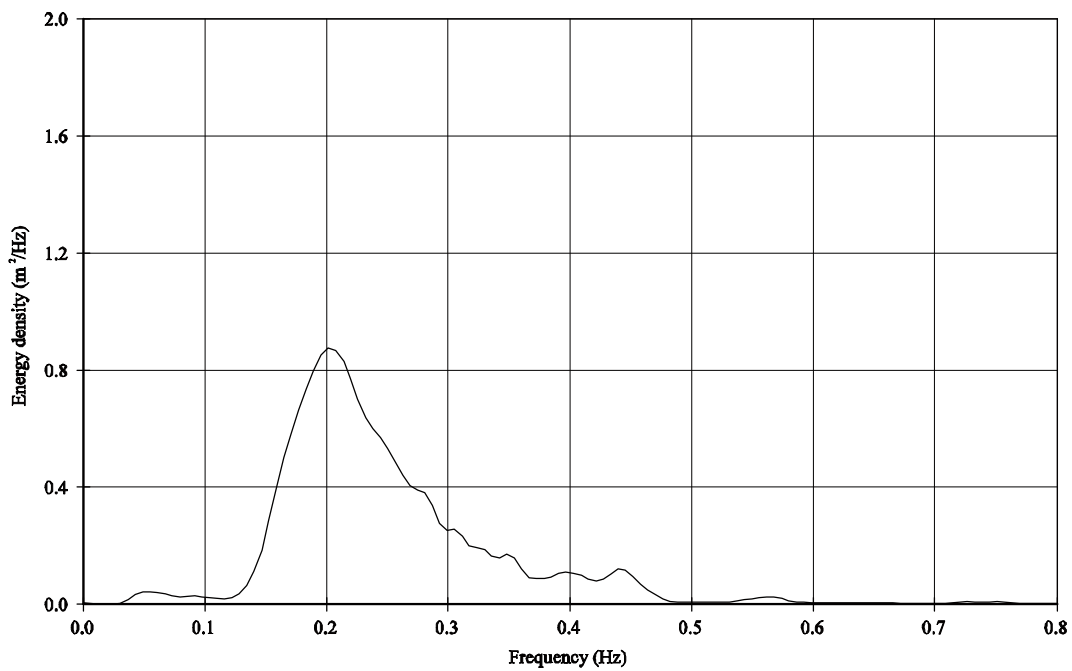
WL/Delft Hydraulics

H4731

Fig. B.12



— Incident



Wave height exceedance curve and
energy density spectrum

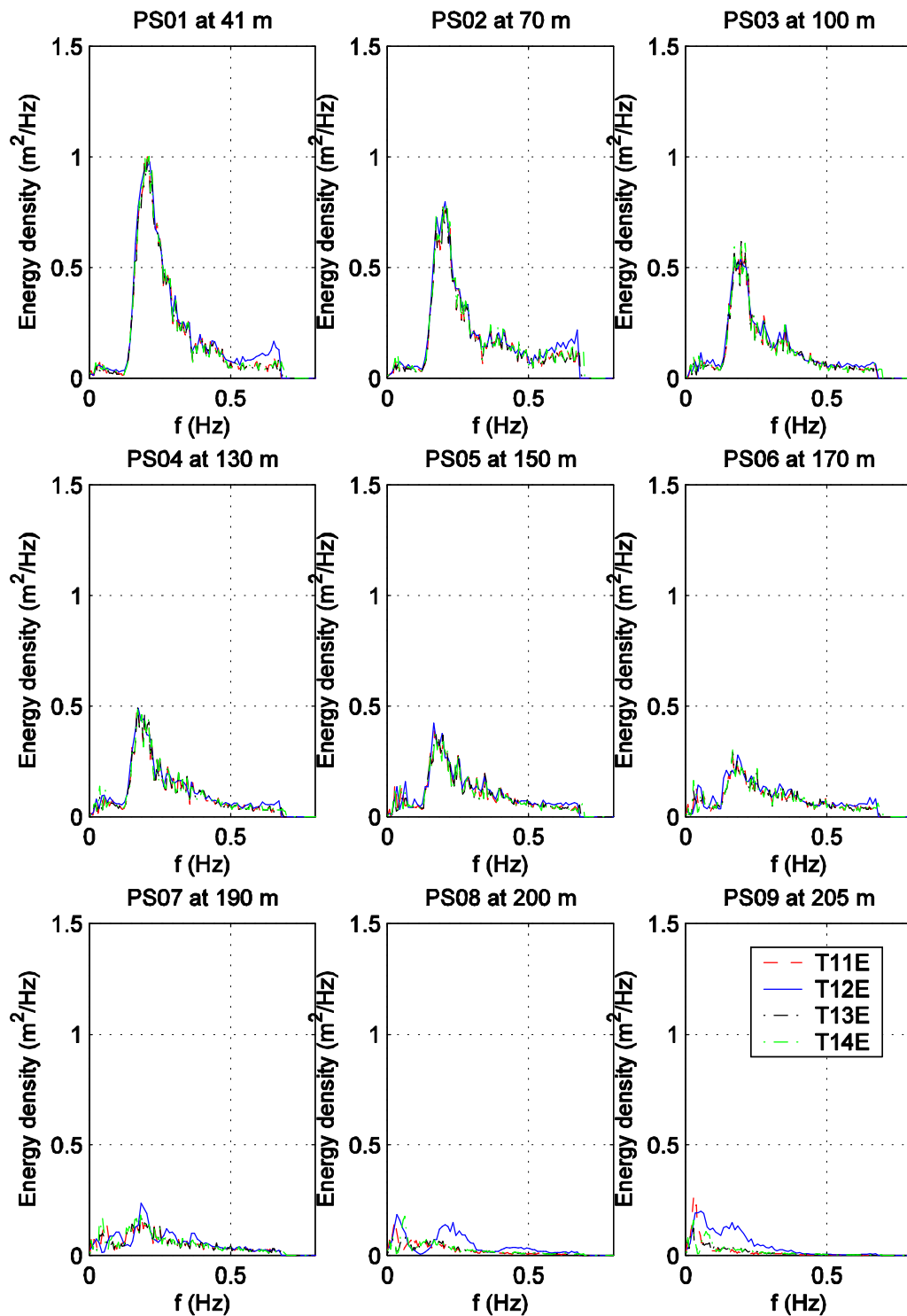
T14E

Incident

WL/Delft Hydraulics

H4731

Fig. B.13



Energy density spectra in pressure sensors

Photographs



Revetment around dune face and dune top before Test T11

a. Revetment during construction



b. Revetment before Test T12



Revetment before Test T12

WL | DELFT HYDRAULICS

H4731

Fig. C.2

a. Revetment during construction



b. Revetment before Test T13



Revetment before Test T13

WL | DELFT HYDRAULICS

H4731

Fig. C.3

a. Dune during construction



b. Dune before Test T14

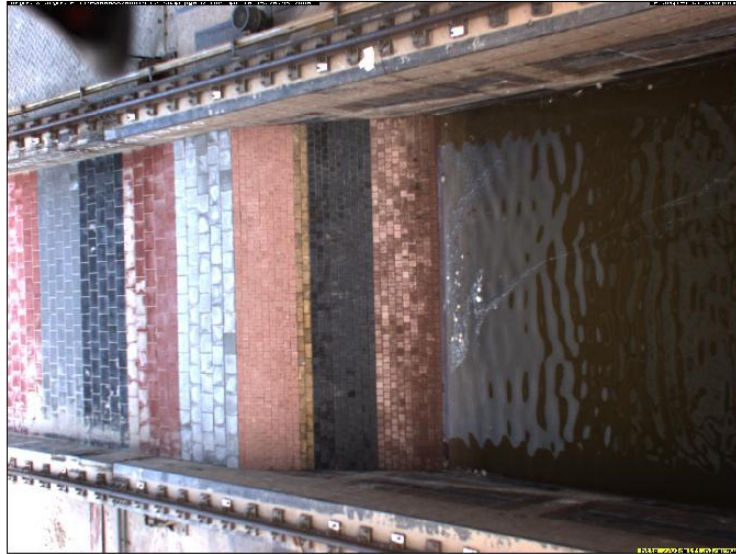


Dune before Test T14

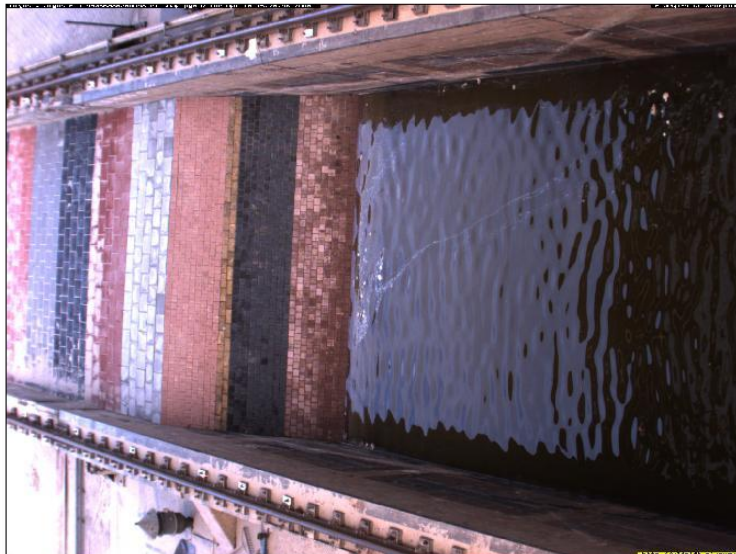


Photograph of amphibious profile follower, flow
velocity meter and pressure sensor

a. CAM 2



b. CAM 1

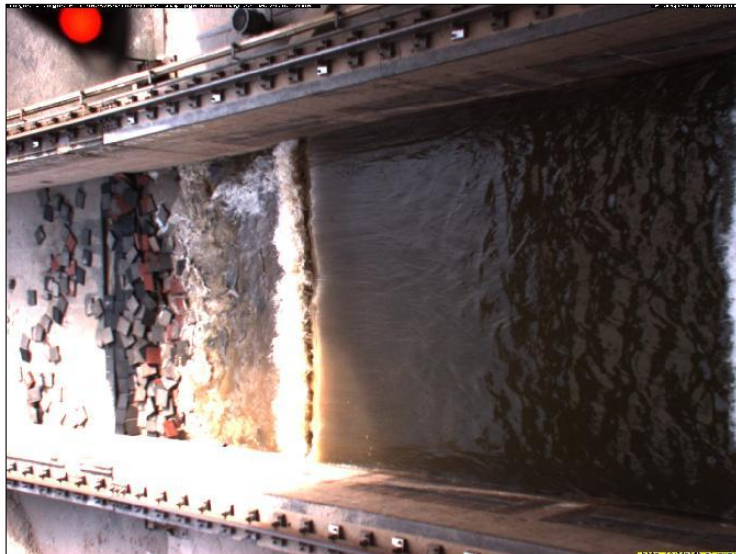


Photographs for stereo video before Test T11

a. CAM 1



b. CAM 2 with LED in upper-left corner turned on

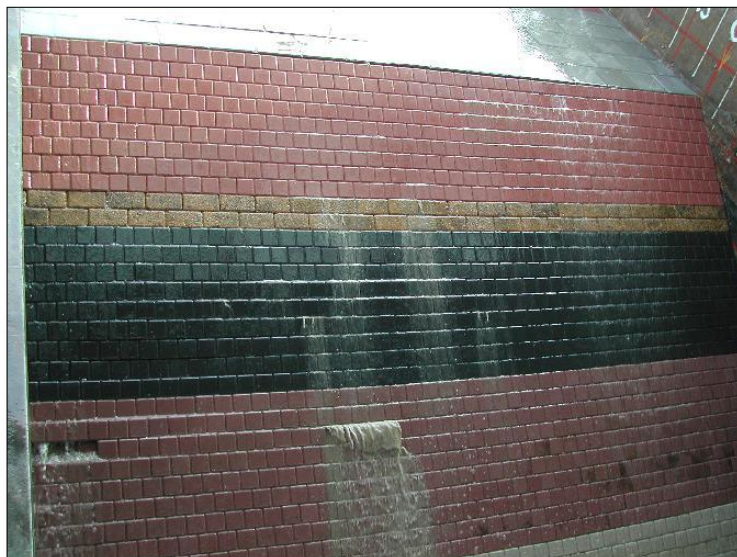


Photographs for stereo video at end of Test T13

a. Wave attack during Test T11A



b. Revetment between two consecutive waves during Test T11B



Wave attack at revetment at beginning of Test T11

a. Wave attack during Test T11C



b. Revetment starts to collapse during Test T11C



Wave attack at revetment during collapse
of revetment on dune face in Test T11

WL | DELFT HYDRAULICS

H4731

Fig. C.9

a. Dune and revetment after Test T11C



b. Dune and revetment after Test T11D



Dune and revetment after collapse of revetment
on dune face in Test T11

WL | DELFT HYDRAULICS

H4731

Fig. C.10

a. Dune and revetment after Test T11E



b. Dune and revetment after Test T11E in dry flume



Dune and revetment after Test T11

WL | DELFT HYDRAULICS

H4731

Fig. C.11

a. Overtopped water on revetment



b. Wave impact at vertical part of revetment



Wave attack at revetment in Test T12

a. Dune and revetment after Test T12



b. Scour hole after Test T12 in dry flume



Dune and revetment after Test T12

a. Dune and revetment during Test T13A



b. Dune and revetment after Test T13B



Wave attack at revetment in Test T13

a. Dune and revetment after Test T13D



b. Dune and revetment after Test T13E



Dune and revetment after Test T13

a. Dune and revetment after Test T13 in dry flume



b. Holes in bed profile around 75 m from wave board



Dune, revetment and bed profile after Test T13 in dry flume

a. Wave attack during Test T14A



b. Dune after Test T14A



Wave attack at dune in Test T14

a. Dune after Test T14C



b. Dune after Test T14E



Dune during and after Test T14

WL | DELFT HYDRAULICS

H4731

Fig. C.18



WL | Delft Hydraulics

Rotterdamseweg 185
postbus 177
2600 MH Delft
telefoon 015 285 85 85
telefax 015 285 85 82
e-mail info@wldelft.nl
internet www.wldelft.nl

Rotterdamseweg 185
p.o. box 177
2600 MH Delft
The Netherlands
telephone +31 15 285 85 85
telefax +31 15 285 85 82
e-mail info@wldelft.nl
internet www.wldelft.nl

